Article

Cell Reports

Macrophages drive KSHV B cell latency

Graphical abstract

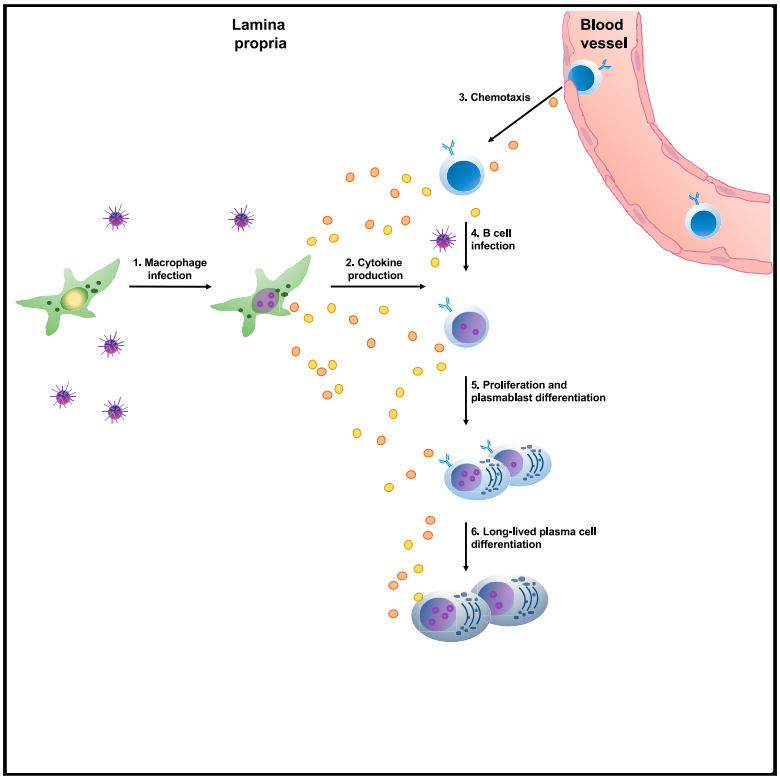

Authors

Agnieszka Szymula, Gabriela Samayoa-Reyes, Sidney Ogolla, ..., Rosemary Rochford, J. Pedro Simas, Kenneth M. Kaye

Correspondence

psimas@medicina.ulisboa.pt (J.P.S.), kkaye@bwh.harvard.edu (K.M.K.)

In brief

Szymula et al. show that Kaposi's sarcoma herpesvirus (KSHV) efficiently infects mononuclear phagocytes, which produce B cell chemoattractants and activating factors. Mononuclear phagocytes stimulate infected B cell differentiation into plasma cells to enable long-term viral latency. Mononuclear phagocytes may underlie the link between malaria and KSHV epidemiology.

Highlights

- KSHV efficiently infects mononuclear phagocytes
- Monocytes and M-CSF macrophages enhance B cell survival and infected B cell proliferation
- M-CSF macrophages drive plasma cell differentiation and long-term KSHV latency
- Patients with malaria have elevated circulating monocytes

Szymula et al., 2023, Cell Reports *42*, 112767
July 25, 2023
https://doi.org/10.1016/j.celrep.2023.112767

CellPress

Cell Reports

CellPress
OPEN ACCESS

Article

Macrophages drive KSHV B cell latency

Agnieszka Szymula,[1,2] Gabriela Samayoa-Reyes,[3] Sidney Ogolla,[4] Bing Liu,[1,2] Shijun Li,[1,2] Athira George,[1,2] Nicholas Van Sciver,[1,2] Rosemary Rochford,[4] J. Pedro Simas,[5,6,*] and Kenneth M. Kaye[1,2,7,8,*]

[1]Departments of Medicine, Brigham and Women's Hospital and Harvard Medical School, Boston, MA 02115, USA
[2]Program in Virology, Harvard Medical School, Boston, MA 02115, USA
[3]Department of Immunology and Microbiology, School of Medicine, University of Colorado, Aurora, CO 80045, USA
[4]Center for Global Health Research, Kenya Medical Research Institute, Kisumu 40100, Kenya
[5]Instituto de Medicina Molecular, Avenida Professor Egas Moniz, 1649-028 Lisboa, Portugal
[6]Católica Biomedical Research, Católica Medical School, Universidade Católica Portuguesa, Palma de Cima, 1649-023 Lisboa, Portugal
[7]Broad Institute of Harvard University and Massachusetts Institute of Technology, Cambridge, MA 02142, USA
[8]Lead contact
*Correspondence: psimas@medicina.ulisboa.pt (J.P.S.), kkaye@bwh.harvard.edu (K.M.K.)
https://doi.org/10.1016/j.celrep.2023.112767

SUMMARY

Kaposi's sarcoma herpesvirus (KSHV) establishes lifelong infection and persists in latently infected B cells. Paradoxically, *in vitro* B cell infection is inefficient, and cells rapidly die, suggesting the absence of necessary factor(s). KSHV epidemiology unexpectedly mirrors that of malaria and certain helminthic infections, while other herpesviruses are ubiquitous. Elevated circulating monocytes are common in these parasitic infections. Here, we show that KSHV infection of monocytes or M-CSF-differentiated (M2) macrophages is highly efficient. Proteomic analyses demonstrate that infection induces macrophage production of B cell chemoattractants and activating factor. We find that KSHV acts with monocytes or M2 macrophages to stimulate B cell survival, proliferation, and plasmablast differentiation. Further, macrophages drive infected plasma cell differentiation and long-term viral latency. In Kenya, where KSHV is endemic, we find elevated monocyte levels in children with malaria. These findings demonstrate a role for mononuclear phagocytes in KSHV B cell latency and suggest that mononuclear phagocyte abundance may underlie KSHV's geographic disparity.

INTRODUCTION

Kaposi sarcoma (KS)-associated herpesvirus (KSHV), a gamma-2 herpesvirus, is the etiologic agent of KS and primary effusion lymphoma (PEL) and is tightly linked with multicentric Castleman's disease (MCD), an aggressive lymphoproliferative disorder. These disorders are most common in immunocompromised individuals, especially those with AIDS.[1] For unknown reasons, and in contrast to other herpesviruses, which are ubiquitous, KSHV epidemiology[2] mirrors that of *Plasmodium falciparum* (*P. falciparum*) malaria and certain helminth infections as evident from multiple epidemiologic studies.[3–7] KSHV prevalence in children is ~63% by age 2 in Kenya, where *P. falciparum* is endemic, and risk of infection increases with higher local malaria infection rates.[8] As a result, seroprevalence is high (~80%) in sub-Saharan Africa but much lower (~5%) in Western nations without similar endemic parasitic infections.[1] Accordingly, KSHV-associated cancer is among the most common malignancies in sub-Saharan Africa, where it is nearly 100-fold more frequent than in high-income nations.[2] KSHV prevalence is also elevated in men who have sex with men (MSMs) (30%–60% seroprevalence) in Europe and the US, but the underlying reasons are also unknown.[9–11]

Similar to other herpesviruses, KSHV infection is lifelong. During latency, KSHV expresses only several of its ~100 open reading frames (ORFs). The latency-associated nuclear antigen (LANA), the predominant viral gene expression product in latent infection, mediates persistence of the multicopy, episomal genome.[12] In infected individuals, KSHV latently persists in infected B cells.[13,14] Paradoxically, however, *in vitro* KSHV infection of B cells is highly inefficient, and cells are short lived.[15–18] KSHV is capable of infecting multiple cell types *in vivo*, including monocytes and macrophages.[19–22]

MCD infected cells exhibit characteristics of B cell plasmablasts, and PEL cells those of plasma cells,[23,24] suggesting that these diseases stem from aberrant development at different stages of infected B cell latency. B cells can differentiate to plasma cells by two primary pathways. In one pathway, B cells differentiate to plasmablasts and long-lived plasma cells by proceeding through a germinal center reaction, in which they undergo somatic hypermutation, thereby producing high-affinity antibody. Alternatively, B cells can progress through an extrafollicular pathway to generate plasma cells. In the latter pathway, somatic hypermutation is typically absent, and low-affinity antibodies are produced.[25,26] MCD and KSHV (alone) infected PEL cells lack somatic hypermutation, suggesting derivation from an extra-follicular pathway.[24,27]

We now find that KSHV infects mononuclear phagocytes with high efficiency and that these cells drive latently infected B cell differentiation to plasmablasts and then long-lived plasma cells. Elevated circulating monocytes is a clinical feature common to parasitic infections epidemiologically linked with KSHV, and,

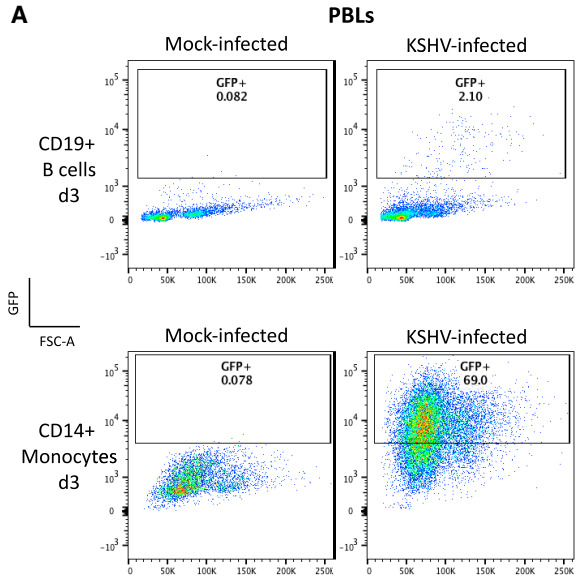

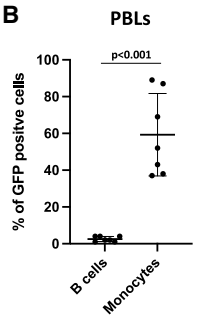

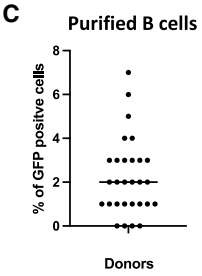

Figure 1. KSHV efficiently infects monocytes

(A and B) PBLs were KSHV infected and assessed by flow cytometry at day 3 post-infection. Dot plots (A) show percentage of infected cells based on viral GFP expression. Data representative of experiments (plotted in B) from 7 independent donor samples on day 3–5 post-infection with MOI ~1–5. Horizontal lines indicate averages, and error bars standard deviation. p values were calculated by two-tailed paired samples t test.

(C) B cells isolated from 29 donor samples were infected with KSHV (or mock infected) with MOI ~1–2 and GFP expression assessed on day 5 post-infection. Horizontal line indicates median.

See also Figure S1.

consistent with these findings, we show that monocytosis occurs in children with symptomatic malaria in Kenya, a KSHV endemic region. Together, these findings provide a potential link between increased mononuclear phagocyte burden and KSHV infection.

RESULTS

KSHV efficiently infects monocytes

We investigated KSHV infection of peripheral blood leukocytes (PBLs). Following incubation with KSHV.219,[28] cells were assessed for infection by detection of GFP, which is constitutively expressed from the recombinant viral genome. Only ~2% of B cells were infected, even after infection of purified B cells (Figures 1A–1C and S1A), and similarly low infection rates occurred in CD4+ T cells, CD8+ T cells, or natural killer (NK) cells (Figures S1C–S1E). In contrast, ~60% of CD14+ monocytes were infected, an efficiency of ~30-fold greater than that of lymphocytes (Figures 1A and 1B). Therefore, KSHV efficiently infects monocytes, but not B cells or other lymphocytes.

Monocytes enhance B cell survival and stimulate KSHV-infected B cell proliferation

Since KSHV efficiently infects monocytes but establishes long-term latency in B cells, we assessed the effect of monocytes on B cell survival and proliferation after infection. In the absence of monocytes, KSHV exerted a small (~25% increase over mock), but significant ($p < 0.001$), survival effect on purified B cells (Figures S2A and S2B), with ~50% of cells surviving at day 5 or 6 post-infection (pi) (Figure S2B, right panel). Since most of the purified B cells are uninfected, increased survival is likely due to pro-survival signals in *trans* from KSHV-infected cells. In contrast, CD19+ B cell survival within PBLs (which include monocytes) was enhanced to nearly 100% regardless of KSHV infection (Figures S2A and S2C). Further, incubation with purified monocytes had a similar effect, with nearly all B cells surviving at day 5 pi (Figures 2A, 2B, and S2G).

We used flow cytometry to assess B cell proliferation, which occurred between days 3 and 6 pi (Figures S2D–S2F). While KSHV alone modestly stimulated infected B cell proliferation (Figures S2E and S2F), monocytes greatly stimulated proliferation of the infected B cells (Figures 2C, 2D, and S2H). In contrast, monocytes did not stimulate proliferation of uninfected B cells (Figures 2C, 2D, and S2H). Therefore, monocytes and KSHV act synergistically to stimulate B cell proliferation.

To assess whether monocyte effects on survival or proliferation are due to soluble factors, we incubated B cells and monocytes in transwell plates (Figure S2I), which physically separate cells but allow transfer of soluble factors. Both survival and infected B cell proliferation were enhanced in this system, though to a lesser degree than with monocyte co-culture (Figures 2, S2G, and S2H). These results indicate that soluble factors are at least partially responsible for enhanced survival and proliferation and that direct contact between monocytes and B cells may be important.

KSHV efficiently infects macrophages and induces B cell chemoattractants

Since monocytes rapidly differentiate upon exiting the bloodstream and entering tissue,[29] where primary KSHV infection likely occurs, we investigated infection of macrophages. Two major categories of macrophages are driven by M-CSF- or GM-CSF-induced monocyte differentiation. M-CSF differentiation (M2 phenotype) occurs constitutively *in vivo*,[30–34] while GM-CSF differentiation (M1 phenotype) does not.[32–36] Therefore, we used M-CSF to differentiate monocytes to macrophages.[37] Similar to monocytes, infection was efficient, based on either GFP or KSHV LANA expression (Figures 3A and 3B), with ~80% of cells infected following infection at a multiplicity of infection (MOI) ~1. In addition to GFP, RFP, under control of the viral early lytic PAN promoter in KSHV.219, was also expressed in infected cells (data not shown). However, we could not detect ORF59, an early lytic gene involved in viral DNA replication, by immune fluorescence microscopy (data not

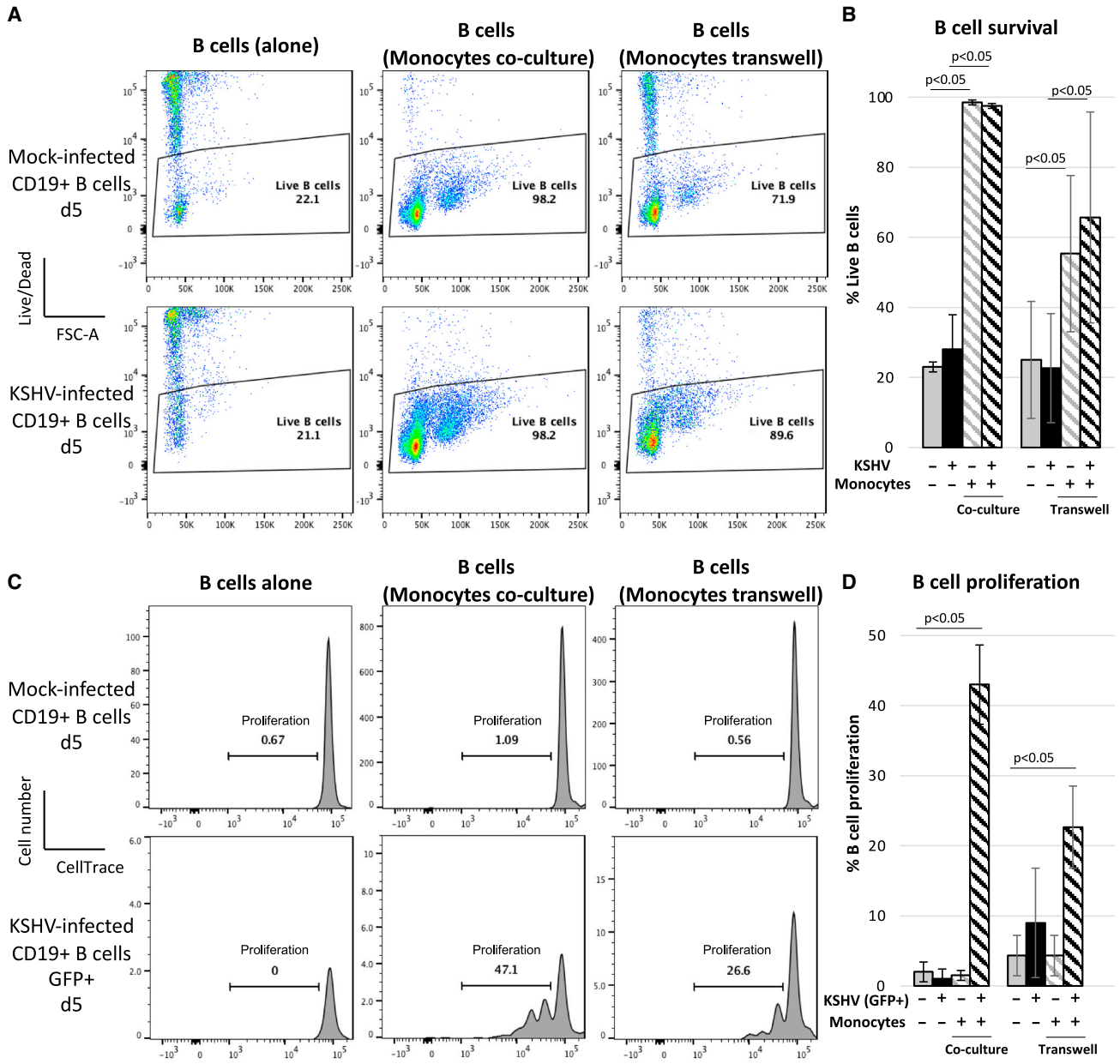

Figure 2. Monocytes increase B cell survival and proliferation

(A and C) Purified B cells cultured alone, with monocytes, or with monocytes in Transwells were infected (or mock infected) at MOI ~1–2 and analyzed by flow cytometry to assess CD19+ B cell viability (A) and proliferation (C).

(B and D) Average percentage of viable (B) or proliferated (D) B cells from 4 independent donor samples (primary data in Figures S2G and S2H). Error bars indicate standard deviation. p values were calculated using t test: one-tailed paired two sample for means.

See also Figure S2.

shown), and no infectious virions were produced (Figure S3A), indicating that despite activity of the PAN promoter, lytic replication was absent. In addition to the viral gene expression, we observed phenotypic differences in infected macrophages, which, in contrast to uninfected cells, began detaching from plates at day ~2–3 pi and underwent slow cell death, with ~50% of infected cells remaining alive at day 5 pi (Figure S3B).

Since soluble factors affected infected cell survival and proliferation (Figure 2), we investigated whether infection alters the macrophage cytokine profile. We assessed a panel of 40 cytokines (Table S1) in cell supernatant and found that ~10% were increased and ~5% decreased at day 3 pi (Figure S3E). The most highly upregulated cytokines were macrophage inflammatory protein (MIP) chemotactic cytokines MIP-1α (CCL3), MIP-1β (CCL4), and MIP-1δ (CCL15 or MIP-5), which were induced ~2-,

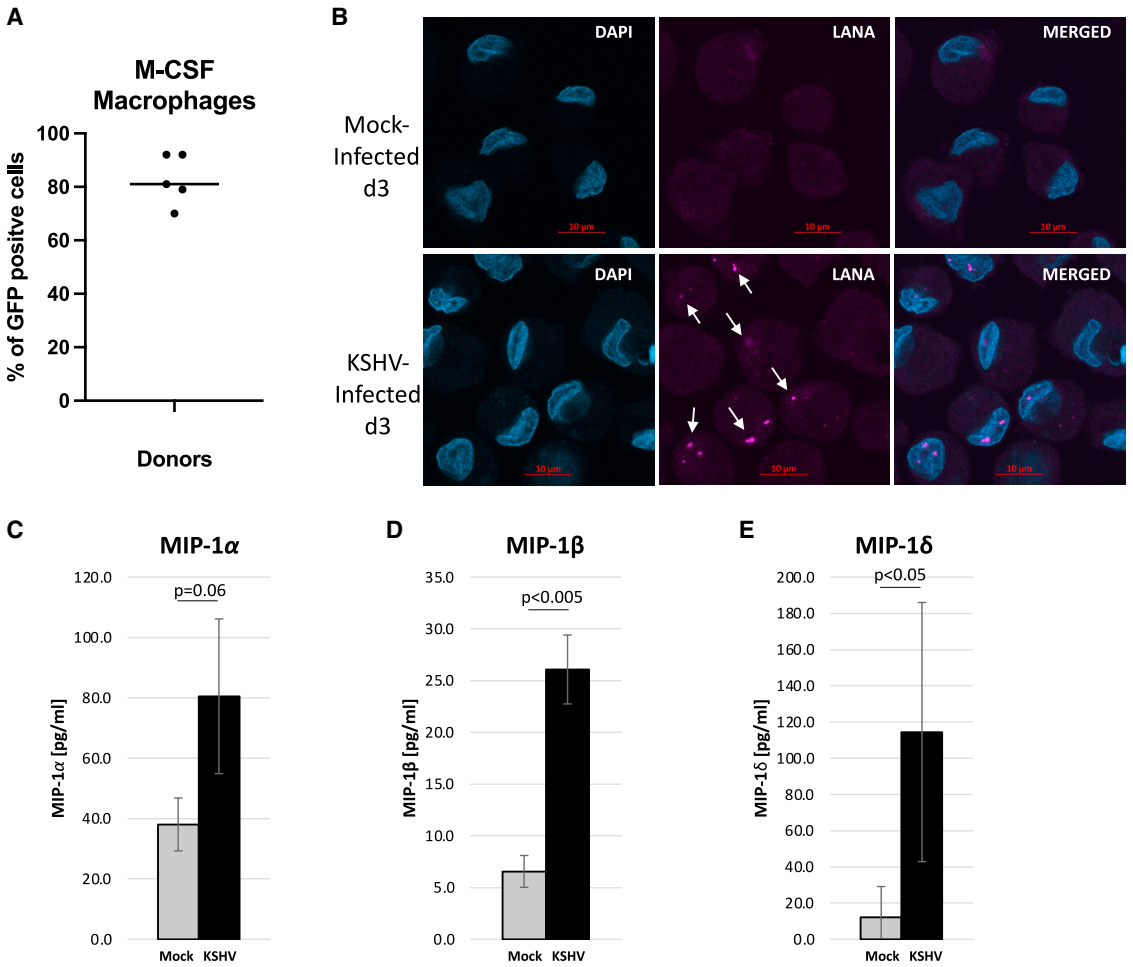

Figure 3. KSHV efficiently infects M-CSF-differentiated macrophages and induces B cell chemoattractants

(A and B) Monocytes were M-CSF differentiated into macrophages and infected with KSHV (or mock infected) at MOI ~1–2.

(A) Infected macrophages from 5 independent donor samples at 5–6 days post-infection as assessed by viral GFP expression. Horizontal line indicates median.

(B) Immune fluorescent microscopy demonstrates LANA (magenta) and DAPI (blue) detection of DNA on day 3 post-infection. Images representative of 5 donor samples. Magnification, 630×. White arrows indicate examples of LANA nuclear dots.

(C–E) Average levels of MIP-1α (C) MIP-1β (D), or MIP-1δ (E) in supernatant of MOI ~1 infected M-CSF-differentiated macrophages from 3 independent donor samples harvested on day 3 post-infection (primary data in Figures S3F–S3H).

Error bars indicate standard deviation. p values were calculated using t test: one-tailed paired two sample for means.

See also Figure S3 and Table S1.

4-, or 10-fold, respectively (Figures 3C–3E and S3F–S3H). Notably, MIP-1α and MIP-1δ are B cell chemoattractants.[38] Therefore, KSHV infection upregulates B cell chemoattractants, consistent with a viral strategy to increase local B cell concentration and infection.

M-CSF macrophages drive infected B cell proliferation and plasmablast differentiation

We examined whether, like monocytes, macrophages promote B cell survival and proliferation. We assessed M-CSF and GM-CSF macrophages differentiated from the same donors. Like monocytes, incubation with M-CSF macrophages (Figure S3I) led to survival of nearly all co-cultured B cells at day 5 pi regardless of infection status (Figures S4A and S4B). Also as with monocytes, M-CSF macrophages greatly stimulated infected B cell proliferation (Figures S4C–S4E). In contrast, incubation with GM-CSF macrophages led to lower B cell survival at ~60%–70% regardless of infection (Figures S4A and S4B), and strikingly, GM-CSF strongly inhibited infected B cell proliferation (Figures S4C and S4D).

Since KSHV-infected B cells in MCD resemble plasmablasts,[39] we assessed if KSHV or macrophages promote B cell plasmablast differentiation by assessing for high-level CD38++ expression in CD19+ cells. No CD38++ cells were present prior to infection of purified B cells (Figure S1B). KSHV led to ~20% of infected cells differentiating to plasmablasts, and co-culture with M-CSF macrophages greatly increased differentiation to over 70% of infected cells at day 5 pi (Figures 4A, 4B, and S5A). In direct contrast, GM-CSF macrophages inhibited all plasmablast differentiation (Figures 4A and S5B). Therefore, KSHV and

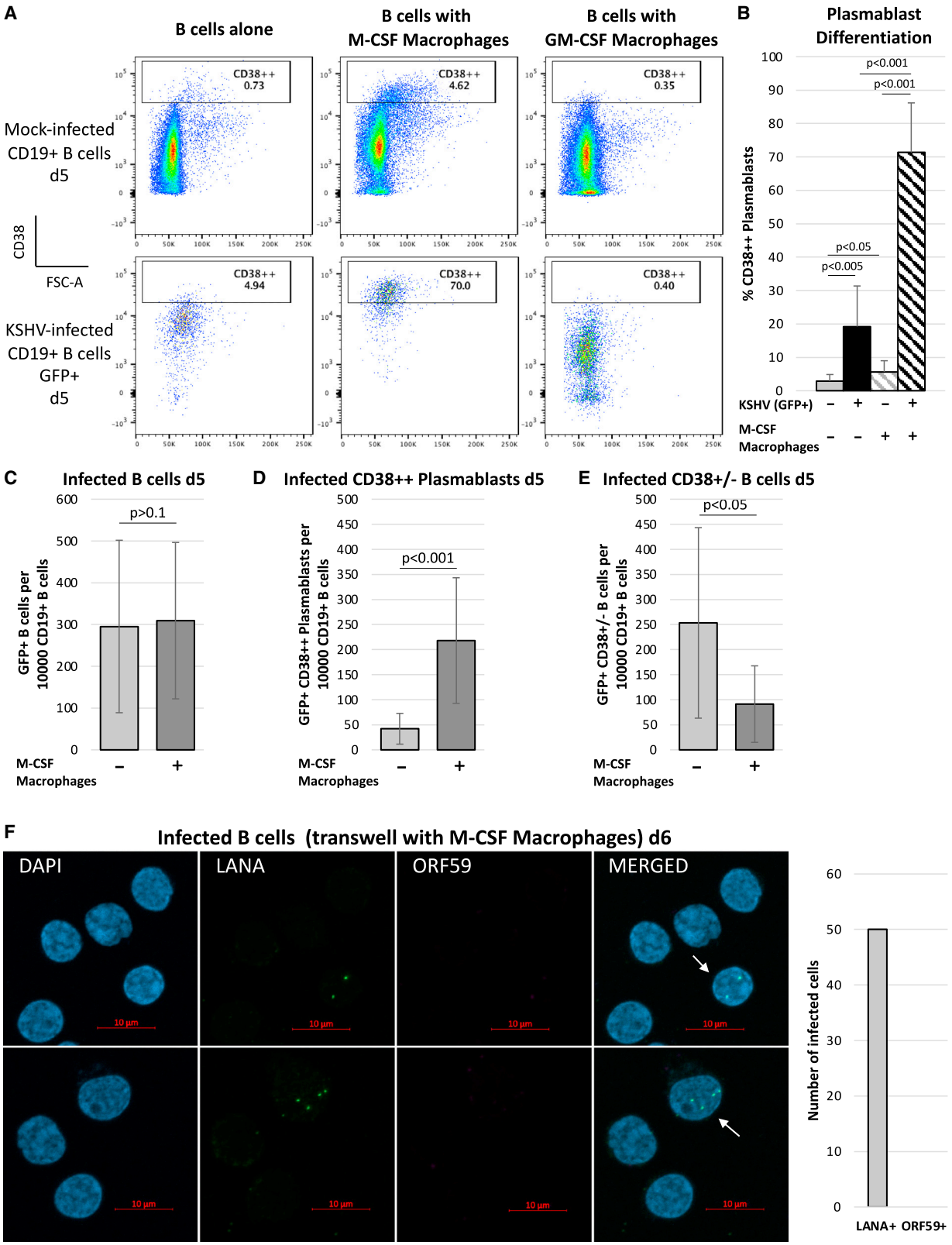

(legend on next page)

M-CSF macrophages act synergistically to stimulate B cell proliferation and plasmablast differentiation.

We assessed frequencies of infected plasmablasts among the total B cell population in the presence or absence of M-CSF macrophages at day 5 pi. While frequencies of infected B cells in either condition were similar (Figures 4C and S5C), in the presence of M-CSF macrophages, infected plasmablast (CD19+CD38++) frequency was 5-fold higher (Figures 4D and S5D), and infected non-plasmablast (CD19+CD38+ or CD19+CD38−) frequency about 3-fold lower (Figures 4E and S5E). These results indicate that differentiation, rather than plasmablast proliferation, primarily accounts for increased plasmablasts when co-cultured with M-CSF macrophages.

We investigated expression of LANA or ORF59 in infected B cells in transwells with M-CSF macrophages by immunofluorescent microscopy at day 6 pi. LANA (green) was present as nuclear dots in numerous infected cells, but no ORF59 was detected (Figure 4F). The absence of ORF59, a lytic protein, indicates these B cells, which include plasmablasts and non-plasmablasts, are latently infected.

KSHV regulates macrophage BAFF and APRIL production

Cytokines B-cell-activating factor (BAFF) and "a proliferation-inducing ligand" (APRIL) contribute to the survival niche of plasmablasts and plasma cells *in vivo*.[40,41] Since BAFF and APRIL were not assessed in the initial cytokine panel, we performed ELISAs for each, which revealed ~4-fold BAFF upregulation (Figure S5F) and ~2-fold APRIL downregulation at day 3 pi (Figure S5G).

We used purified BAFF or APRIL to assess effects on infected B cells. While BAFF promoted plasmablast differentiation of infected B cells (Figures S5H and S5I), APRIL had no significant effect (Figures S5H and S5I). Since BAFF and APRIL compete for binding to common receptors,[42] KSHV upregulation of BAFF and downregulation of APRIL are expected to promote infected B cell differentiation.

M-CSF macrophages drive plasma cell differentiation and long-term KSHV latency

PEL cells exhibit plasma cell features, suggesting they derive from aberrant events in latently infected plasma cells.[39] Since M-CSF macrophages drive infected plasmablast differentiation, we asked if they also drive further differentiation into plasma cells. Plasma cell differentiation typically occurs over days to weeks, during which B cells gain the CD138 surface marker.[43–45] We incubated infected B cells with M-CSF macrophages for 42 days. During this time, infected macrophages were replenished weekly due to their slow death following infection (Figure S3B). (These infected macrophages did not transfer additional virus to B cells [Figures S3C and S3D].) Since plasma cells typically do not express CD19 and CD20,[25,46] we used the absence of CD14 to identify B cells (as the experiment included only B cells and macrophages). As expected, CD38++ plasmablast differentiation occurred in ~40% of infected B cells at 5 days pi (Figures 5A, 5B, and S6A). However, subsequently, there was progressive loss of CD38++ at days 21 and 42 pi, with loss of nearly all plasmablasts by day 42 (Figures 5A, 5B, and S6A). Strikingly, in parallel with CD38++ loss, greater than 50% of infected cells differentiated into CD138+ plasma cells by day 42 (Figures 5A, 5C, and S6B). In contrast, uninfected cells did not differentiate into plasma cells in the presence of infected macrophages (Figures 5A, 5C, and S6B).

We also assessed cell numbers for each time point of the experiment. While total B cells decreased during the time course (Figure S6C), infected cell numbers remained stable, or only modestly decreased, for all but one donor (Figure S6D). Among these donors with stable, infected cell numbers, KSHV-infected plasma cells increased ~2- to 12-fold (Figure S6F), while uninfected plasma cell numbers remained unchanged (Figure S6E). Together, these results demonstrate that M-CSF macrophages actively drive infected B cell differentiation into plasma cells, where KSHV establishes long-term latency.

Elevated circulating monocytes in acute malaria in a KSHV endemic region

KSHV endemicity parallels that of *P. falciparum* malaria and certain helminthic infections.[3,4,6,47] Increased circulating monocytes are a clinical feature common to these parasitic infections.[48–54] In Kenya, *P. falciparum* malaria and KSHV are frequent in young children. We therefore assessed circulating monocyte levels in PBLs in Kenyan children aged 1–5 years (Table S2). Children with clinically symptomatic malaria had markedly elevated monocytes compared with controls (Figure 6A). This finding was specific to monocytes since B cell levels were similar between the groups (Figure 6B).

DISCUSSION

These findings demonstrate a central role for mononuclear phagocytes in driving infected B cell proliferation and differentiation to plasma cells, in which KSHV establishes long-term,

Figure 4. M-CSF macrophages drive B cell plasmablast differentiation

(A) Purified B cells alone or co-cultured with M-CSF or GM-CSF macrophages were infected with KSHV (or mock infected) at MOI ~1–2 and assessed at 5 days post-infection for CD38++ expression. Plots gated on live CD19+ B cells (mock infected) or live CD19+GFP+ B cells (KSHV infected). Data representative of 2 independent donor experiments (see Figure S5B).

(B) Average percentage plasmablast differentiated cells following KSHV infection at MOI ~1–2 from 9 independent donor samples with or without M-CSF macrophage co-culture at day 5 post-infection (primary data in Figure S5A). Error bars indicate standard deviation. p values calculated using t test: one-tailed paired two sample for means.

(C–E) Frequencies of infected (GFP+) CD19+ B cells (C), infected CD38++ plasmablasts (D), or infected CD38+/− B cells (E) per 10,000 CD19+ B cells, averaged from 10 independent B cell donor samples on day 5 post-infection (primary data in Figures S5C–S5E).

(F) Immune fluorescent microscopy detecting LANA (green), ORF59 (magenta), and DAPI (blue) staining of DNA on day 6 post-infection of purified B cells in Transwells with M-CSF macrophages. Magnification, 630×. Orthogonal projections of z stacks are shown. Arrows indicate cells expressing LANA. Numbers of cells expressing LANA and ORF59 are shown at right.

See also Figures S1 and S5.

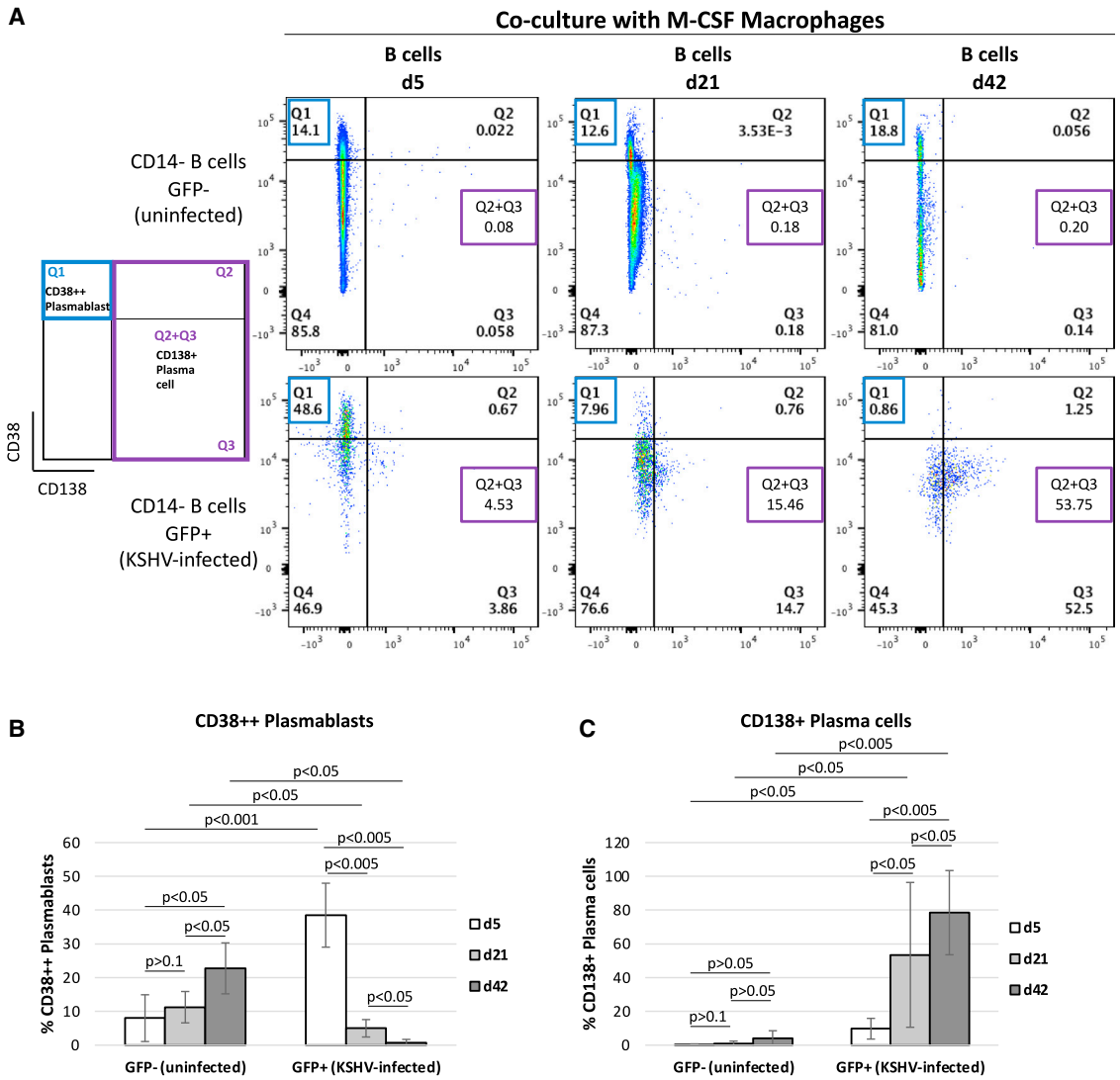

Figure 5. M-CSF macrophages drive KSHV-infected B cell differentiation into long-lived plasma cells

(A–C) B cells co-cultured with M-CSF macrophages were infected with KSHV at MOI ~1.

(A) Cells were assessed by flow cytometry for percentage of CD38++ plasmablasts (Q1) or CD138+ plasma cells (Q2+Q3). CD14+ cells (macrophages) were gated out to limit analyses to B cells (Figure S3J). Data are representative of 4 independent donor sample experiments (primary data in Figures S6A–S6F).

(B and C) Average percentage of CD38++ plasmablasts (B) or CD138+ plasma cells (C) at indicated day post-infection with M-CSF macrophage co-culture. Error bars indicate standard deviation. p values calculated using t test: one-tailed paired two sample for means.

See also Figure S6.

latent infection (Figure 6C). Virus from saliva, the vehicle of KSHV transmission,[55] that gains access to submucosal tissue (e.g., through disruptions in the epithelial layer, lytic replication in epithelial cells, or directly traversing epithelial cells) rich in M-CSF macrophage cells, such as in the lamina propria of the oral cavity following saliva exposure,[56] would lead to infected macrophage chemoattractant release to increase local B cell concentration and infection. Such recruitment and subsequent macrophage-driven expansion of infected cells may therefore overcome innate low-level B cell infectivity and allow latent infection to be established. Further, these findings support the derivation of the pathologic cells in MCD (plasmablasts) or PEL (plasma cells) from different stages of infected B cell maturation and show that KSHV B cell infection, in concert with infected macrophages, effectively substitutes for the multiple exogenous factors, including BAFF, APRIL, CD40L, CpG, and interleukin-6 (IL-6), otherwise required for *in vitro* plasma cell differentiation.[40,41,43]

Consistent with these findings, prior work demonstrated that KSHV infection of primary B cells induced plasmablast morphology.[18] Other work described preferential KSHV infection of plasma cells, although KSHV-driven B cell differentiation into plasma cells was not excluded.[17] Co-infection with Epstein-Barr virus (EBV), a gamma-1 herpesvirus, which occurs in most, but

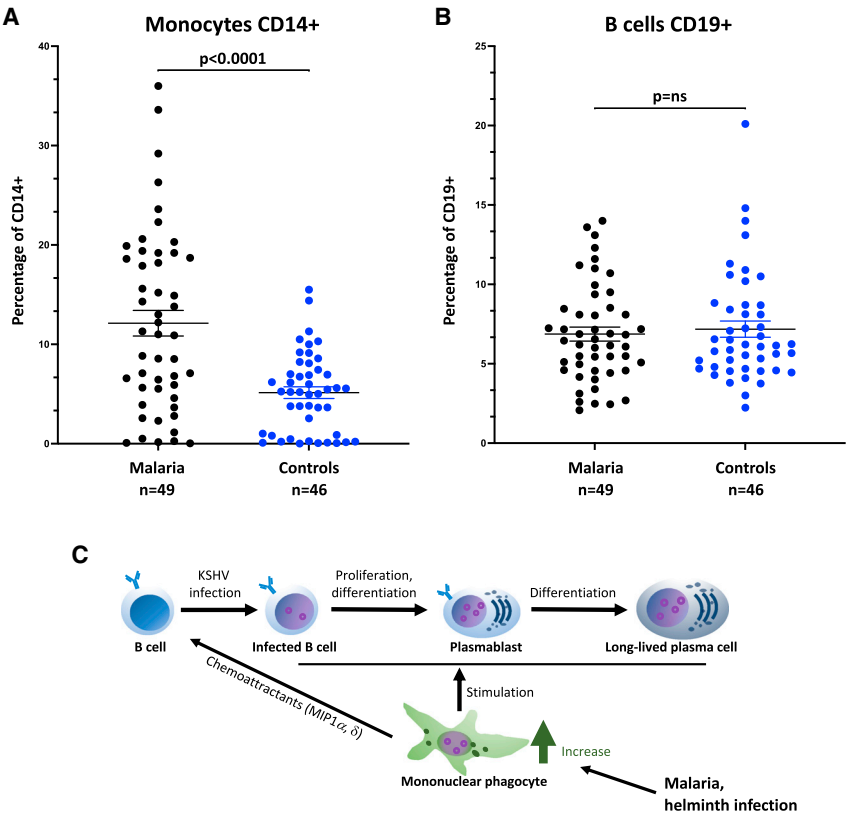

Figure 6. Elevated blood monocytes in Kenyan children with malaria

(A and B) PBLs from 49 Kenyan children with malaria or 46 controls (Table S2) were assessed by flow cytometry for the percentage of (A) CD14+ monocytes or (B) CD19+ B cells. Horizontal lines indicate mean, error bars indicate standard error of the mean (SEM), and p values calculated using unpaired t test. (C) Model of mononuclear phagocyte driven infected B cell plasma cell differentiation.

not all, PEL tumors, appears capable of substituting for mononuclear phagocytes to allow long-term B cell persistence of KSHV, likely due to EBV's B cell transformation ability.[57,58] KSHV and EBV co-infection of humanized mice resulted in co-infected plasma cell-like cells,[59] and efficient KSHV persistence in these mice required the presence of EBV. Our results suggest that the requirement for EBV may relate to the deficiency of myeloid cells (including mononuclear phagocytes) in humanized mice models.[60]

The absence of somatic hypermutation in MCD and EBV negative PEL[23,24,27] suggests infected plasma cell differentiation outside of the germinal center, consistent with our findings. In contrast, EBV drives B cell differentiation through a germinal center reaction,[61] and the related gammaherpesvirus, murine gammaherpesvirus 68 (MHV68), drives germinal center B cell proliferation in mice.[62] Notably, prior to B cell infection, MHV68 infects macrophages to acquire viral surface glycoproteins that allow efficient B cell infection.[63] Although KSHV infects monocytes and macrophages and expresses lytic genes,[64,65] we did not detect virus production from these cells, suggesting that KSHV gains B cell entry differently from MHV68.

These results suggest a mechanistic link underlying KSHV's unusual epidemiology where mononuclear phagocytes promote infected B cell survival, proliferation, and differentiation to drive viral latency. Consistent with earlier work,[48–51] we find monocytosis in children with acute malaria (Figure 6A). BAFF is elevated in *P. falciparum* malaria,[66,67] providing conditions conducive for KSHV plasma cell latency establishment. M2 monocyte polarization is present in children with *P. falciparum* malaria, and M2 macrophages are induced in a mouse model of cerebral malaria,[68,69] further indicating an environment highly favorable for KSHV latency. Intriguingly, infection with the parasite *Trichostrongylus* is associated with decreased KSHV seroprevalence,[3] and this parasite decreases, rather than increases, monocyte levels.[70]

In endemic regions, *P. falciparum* infection occurs frequently in young children, in whom KSHV infection is common.[8] KSHV infection is expected to occur from exposure to saliva from individuals who are shedding virus during various caregiving practices, including premasticating food or inserting a finger lubricated with saliva into a child's rectum to relieve constipation.[71] As KSHV exposure is expected to be intermittent, frequent malarial illness increases the likelihood of KSHV exposure at a time of increased mononuclear phagocyte burden. However, direct support for elevated mononuclear phagocytes leading to KSHV infection will likely require a large, prospective trial and will be complicated by KSHV's delayed (up to several weeks) seroconversion following exposure and seroreversion, which is common in children.[8,72]

This work demonstrates that M2 (M-CSF-differentiated), but not M1 (GM-CSF-differentiated), macrophages drive KSHV-infected B cell proliferation and differentiation. Prior work showed that KSHV infection of macrophages, or co-culture of macrophages with supernatant from KSHV-infected endothelial cells, skews macrophages to an M2 phenotype.[73,74] In addition, infected macrophages enhanced KSHV tumor growth in a nude mouse model.[74] Although M2 macrophages are present in KS lesions,[19] they occur at lower frequency than in adjacent, uninvolved tissue, while M1 macrophages are randomly distributed, suggesting a different role for M2 macrophages in KS (a spindle cell tumor) compared with primary B cell infection.

KSHV's dependence on mononuclear phagocytic cells also provides a potential explanation for KSHV's high prevalence among MSMs, which sharply contrasts with the general population in Western nations.[9–11] Receptive anal intercourse may lead to microtrauma of rectal mucosal epithelium with exposure of underlying lamina propria, where a rich population of macrophages resides.[75–78] Insertive rimming (oral-anal contact) is

common among MSMs and is associated with KSHV infection.[79,80] Virus in saliva would thus provide access to rectal macrophages.

In summary, this work describes an important role of mononuclear phagocytes in facilitating establishment of viral latency in B cells. Mononuclear phagocytes stimulate survival, proliferation, and differentiation of infected B cells, overcoming the obstacles of inefficient B cell infection and early cell death observed *in vitro* and leading to long-term latency. This dependence on mononuclear phagocytes may provide an explanation for the epidemiology of KSHV, which mirrors that of *P. falciparum* malaria and certain helminthic diseases. Future work further exploring the mechanisms underlying KSHV B cell latency establishment, and further investigating the link between elevated mononuclear phagocyte burden and KSHV infection, should provide new insight into KSHV biology.

Limitations of the study

The use of human subject samples in this work presented certain limitations. First, sample size of PBL-sourced experiments was affected because of the limited availability of donors. In addition, PBL donors were anonymized and clinical information unavailable. Therefore, potential factors, such as recent illness or vaccination, may have introduced effects that cannot be accounted for. Similarly, little clinical information was available for the patients with malaria or the control subjects. Last, as noted above, definitive investigation of the link between elevated mononuclear phagocytes in certain parasitic infections and a predisposition to KSHV infection will likely require a large, prospective trial.

STAR★METHODS

Detailed methods are provided in the online version of this paper and include the following:

- KEY RESOURCES TABLE
- RESOURCE AVAILABILITY
  - Lead contact
  - Materials availability
  - Data and code availability
- EXPERIMENTAL MODEL AND SUBJECT DETAILS
  - Human studies
  - Primary cells
  - Cell lines
- METHOD DETAILS
  - PBL isolation
  - Differentiation of monocytes into macrophages
  - Virus production and titration
  - Flow cytometry staining and gating
  - Immunofluorescence microscopy
  - Cytokine detection assays
  - Virus infections of cells and co-cultures
  - Cytokine stimulation assays
  - Assessment of KSHV production from infected macrophages
  - Collection and assessment of PBLs from Kenya
- QUANTIFICATION AND STATISTICAL ANALYSIS

SUPPLEMENTAL INFORMATION

Supplemental information can be found online at https://doi.org/10.1016/j.celrep.2023.112767.

ACKNOWLEDGMENTS

We thank Bala Chandran for the anti-ORF59 11D1 antibody. This work was supported in part by National Institutes of Health grants AI150575, DE025208, and AI165382 to K.M.K., the Department of Immunology and Microbiology pilot funding, CU Anschutz, NIH R01 AI 1141531 and R01 CA239588 to R.R., NIH T32 AI007245 to N.V.S., and Fundação para a Ciência e Tecnologia Grant PTDC/BIA-VIR/27947/2017 to J.P.S.

AUTHOR CONTRIBUTIONS

Study design, A.S., J.P.S., and K.M.K.; experimental work, A.S.; data interpretation, A.S., B.L., S.L., A.G., N.V.S., R.R., J.P.S., and K.M.K.; writing, A.S., J.P.S., and K.M.K.; paper review, A.S., J.P.S., K.M.K., B.L., S.L., A.G., N.V.S., G.S.-R., and R.R.; collection and analysis of malaria and control samples from Kenya, G.S.-R.; collection of malaria and control PBLs in Kenya, S.O.; collection of acute malaria and control PBLs in Kenya, R.R.

DECLARATION OF INTERESTS

The authors declare no competing interests.

INCLUSION AND DIVERSITY

We support inclusive, diverse, and equitable conduct of research.

Received: February 3, 2023
Revised: June 6, 2023
Accepted: June 22, 2023

REFERENCES

1. Cesarman, E., Damania, B., Krown, S.E., Martin, J., Bower, M., and Whitby, D. (2019). Kaposi sarcoma. Nat. Rev. Dis. Primers *5*, 9. https://doi.org/10.1038/s41572-019-0060-9.
2. Rebbeck, T.R. (2020). Cancer in sub-Saharan Africa. Science *367*, 27–28. https://doi.org/10.1126/science.aay4743.
3. Wakeham, K., Webb, E.L., Sebina, I., Muhangi, L., Miley, W., Johnson, W.T., Ndibazza, J., Elliott, A.M., Whitby, D., and Newton, R. (2011). Parasite infection is associated with Kaposi's sarcoma associated herpesvirus (KSHV) in Ugandan women. Infect. Agent. Cancer *6*, 15. https://doi.org/10.1186/1750-9378-6-15.
4. Wakeham, K., Webb, E.L., Sebina, I., Nalwoga, A., Muhangi, L., Miley, W., Johnston, W.T., Ndibazza, J., Whitby, D., Newton, R., and Elliott, A.M. (2013). Risk factors for seropositivity to Kaposi sarcoma-associated herpesvirus among children in Uganda. J. Acquir. Immune Defic. Syndr. *63*, 228–233. https://doi.org/10.1097/QAI.0b013e31828a7056.
5. Nalwoga, A., Cose, S., Wakeham, K., Miley, W., Ndibazza, J., Drakeley, C., Elliott, A., Whitby, D., and Newton, R. (2015). Association between malaria exposure and Kaposi's sarcoma-associated herpes virus seropositivity in Uganda. Trop. Med. Int. Health *20*, 665–672. https://doi.org/10.1111/tmi.12464.
6. Nalwoga, A., Cose, S., Nash, S., Miley, W., Asiki, G., Kusemererwa, S., Yarchoan, R., Labo, N., Whitby, D., and Newton, R. (2018). Relationship Between Anemia, Malaria Coinfection, and Kaposi Sarcoma-Associated Herpesvirus Seropositivity in a Population-Based Study in Rural Uganda. J. Infect. Dis. *218*, 1061–1065. https://doi.org/10.1093/infdis/jiy274.
7. Sabourin, K.R., Daud, I., Ogolla, S., Labo, N., Miley, W., Lamb, M., Newton, R., Whitby, D., and Rochford, R. (2021). Malaria is associated

with Kaposi sarcoma-associated herpesvirus (KSHV) seroconversion in a cohort of western Kenyan children. J. Infect. Dis. *224*, 303–311. https://doi.org/10.1093/infdis/jiaa740.

8. Sabourin, K.R., Daud, I., Ogolla, S., Labo, N., Miley, W., Lamb, M., Newton, R., Whitby, D., and Rochford, R. (2021). Malaria Is Associated With Kaposi Sarcoma-Associated Herpesvirus Seroconversion in a Cohort of Western Kenyan Children. J. Infect. Dis. *224*, 303–311. https://doi.org/10.1093/infdis/jiaa740.
9. Martin, J.N., Ganem, D.E., Osmond, D.H., Page-Shafer, K.A., Macrae, D., and Kedes, D.H. (1998). Sexual transmission and the natural history of human herpesvirus 8 infection. N. Engl. J. Med. *338*, 948–954.
10. Smith, N.A., Sabin, C.A., Gopal, R., Bourboulia, D., Labbet, W., Boshoff, C., Barlow, D., Band, B., Peters, B.S., de Ruiter, A., et al. (1999). Serologic evidence of human herpesvirus 8 transmission by homosexual but not heterosexual sex. J. Infect. Dis. *180*, 600–606. https://doi.org/10.1086/314926.
11. Phillips, A.M., Jones, A.G., Osmond, D.H., Pollack, L.M., Catania, J.A., and Martin, J.N. (2008). Awareness of Kaposi's sarcoma-associated herpesvirus among men who have sex with men. Sex. Transm. Dis. *35*, 1011–1014. https://doi.org/10.1097/OLQ.0b013e318182c91f.
12. Ballestas, M.E., Chatis, P.A., and Kaye, K.M. (1999). Efficient persistence of extrachromosomal KSHV DNA mediated by latency- associated nuclear antigen. Science *284*, 641–644.
13. Whitby, D., Howard, M.R., Tenant-Flowers, M., Brink, N.S., Copas, A., Boshoff, C., Hatzioannou, T., Suggett, F.E., Aldam, D.M., Denton, A.S., et al. (1995). Detection of Kaposi sarcoma associated herpesvirus in peripheral blood of HIV-infected individuals and progression to Kaposi's sarcoma [see comments]. Lancet *346*, 799–802.
14. Ambroziak, J.A., Blackbourn, D.J., Herndier, B.G., Glogau, R.G., Gullett, J.H., McDonald, A.R., Lennette, E.T., and Levy, J.A. (1995). Herpes -Like Sequences in HIV-Infected and Uninfected kaposi's Sarcoma Patients. Science *268*, 582–583.
15. Nicol, S.M., Sabbah, S., Brulois, K.F., Jung, J.U., Bell, A.I., and Hislop, A.D. (2016). Primary B Lymphocytes Infected with Kaposi's Sarcoma-Associated Herpesvirus Can Be Expanded In Vitro and Are Recognized by LANA-Specific CD4+ T Cells. J. Virol. *90*, 3849–3859. https://doi.org/10.1128/JVI.02377-15.
16. Myoung, J., and Ganem, D. (2011). Active lytic infection of human primary tonsillar B cells by KSHV and its noncytolytic control by activated CD4+ T cells. J. Clin. Invest. *121*, 1130–1140. https://doi.org/10.1172/JCI43755.
17. Aalam, F., Nabiee, R., Castano, J.R., and Totonchy, J. (2020). Analysis of KSHV B lymphocyte lineage tropism in human tonsil reveals efficient infection of CD138+ plasma cells. PLoS Pathog. *16*, e1008968. https://doi.org/10.1371/journal.ppat.1008968.
18. Hassman, L.M., Ellison, T.J., and Kedes, D.H. (2011). KSHV infects a subset of human tonsillar B cells, driving proliferation and plasmablast differentiation. J. Clin. Invest. *121*, 752–768. https://doi.org/10.1172/JCI44185.
19. Lidenge, S.J., Tso, F.Y., Ngalamika, O., Kolape, J., Ngowi, J.R., Mwaiselage, J., Wood, C., and West, J.T. (2020). Lack of CD8(+) T-cell co-localization with Kaposi's sarcoma-associated herpesvirus infected cells in Kaposi's sarcoma tumors. Oncotarget *11*, 1556–1572. https://doi.org/10.18632/oncotarget.27569.
20. Henry, M., Uthman, A., Geusau, A., Rieger, A., Furci, L., Lazzarin, A., Lusso, P., and Tschachler, E. (1999). Infection of circulating CD34+ cells by HHV-8 in patients with Kaposi's sarcoma. J. Invest. Dermatol. *113*, 613–616. https://doi.org/10.1046/j.1523-1747.1999.00733.x.
21. Pellet, C., Kerob, D., Dupuy, A., Carmagnat, M.V., Mourah, S., Podgorniak, M.P., Toledano, C., Morel, P., Vérola, O., Dosquet, C., et al. (2006). Kaposi's sarcoma-associated herpesvirus viremia is associated with the progression of classic and endemic Kaposi's sarcoma. J. Invest. Dermatol. *126*, 621–627. https://doi.org/10.1038/sj.jid.5700083.
22. Blasig, C., Zietz, C., Haar, B., Neipel, F., Esser, S., Brockmeyer, N.H., Tschachler, E., Colombini, S., Ensoli, B., and Stürzl, M. (1997). Monocytes in Kaposi's sarcoma lesions are productively infected by human herpesvirus 8. J. Virol. *71*, 7963–7968. https://doi.org/10.1128/JVI.71.10.7963-7968.1997.
23. Du, M.Q., Liu, H., Diss, T.C., Ye, H., Hamoudi, R.A., Dupin, N., Meignin, V., Oksenhendler, E., Boshoff, C., and Isaacson, P.G. (2001). Kaposi sarcoma-associated herpesvirus infects monotypic (IgM lambda) but polyclonal naive B cells in Castleman disease and associated lymphoproliferative disorders. Blood *97*, 2130–2136.
24. Chadburn, A., Hyjek, E.M., Tam, W., Liu, Y., Rengifo, T., Cesarman, E., and Knowles, D.M. (2008). Immunophenotypic analysis of the Kaposi sarcoma herpesvirus (KSHV; HHV-8)-infected B cells in HIV+ multicentric Castleman disease (MCD). Histopathology *53*, 513–524. https://doi.org/10.1111/j.1365-2559.2008.03144.x.
25. Khodadadi, L., Cheng, Q., Radbruch, A., and Hiepe, F. (2019). The Maintenance of Memory Plasma Cells. Front. Immunol. *10*, 721. https://doi.org/10.3389/fimmu.2019.00721.
26. Wilmore, J.R., and Allman, D. (2017). Here, There, and Anywhere? Arguments for and against the Physical Plasma Cell Survival Niche. J. Immunol. *199*, 839–845. https://doi.org/10.4049/jimmunol.1700461.
27. Matolcsy, A., Nádor, R.G., Cesarman, E., and Knowles, D.M. (1998). Immunoglobulin VH gene mutational analysis suggests that primary effusion lymphomas derive from different stages of B cell maturation. Am. J. Pathol. *153*, 1609–1614. https://doi.org/10.1016/S0002-9440(10)65749-5.
28. Vieira, J., and O'Hearn, P.M. (2004). Use of the red fluorescent protein as a marker of Kaposi's sarcoma-associated herpesvirus lytic gene expression. Virology *325*, 225–240. https://doi.org/10.1016/j.virol.2004.03.049.
29. Italiani, P., and Boraschi, D. (2014). From Monocytes to M1/M2 Macrophages: Phenotypical vs. Functional Differentiation. Front. Immunol. *5*, 514. https://doi.org/10.3389/fimmu.2014.00514.
30. Chitu, V., and Stanley, E.R. (2006). Colony-stimulating factor-1 in immunity and inflammation. Curr. Opin. Immunol. *18*, 39–48. https://doi.org/10.1016/j.coi.2005.11.006.
31. Hamilton, J.A. (2008). Colony-stimulating factors in inflammation and autoimmunity. Nat. Rev. Immunol. *8*, 533–544. https://doi.org/10.1038/nri2356.
32. Burgess, A.W., and Metcalf, D. (1980). The nature and action of granulocyte-macrophage colony stimulating factors. Blood *56*, 947–958.
33. Fleetwood, A.J., Lawrence, T., Hamilton, J.A., and Cook, A.D. (2007). Granulocyte-macrophage colony-stimulating factor (CSF) and macrophage CSF-dependent macrophage phenotypes display differences in cytokine profiles and transcription factor activities: implications for CSF blockade in inflammation. J. Immunol. *178*, 5245–5252. https://doi.org/10.4049/jimmunol.178.8.5245.
34. Verreck, F.A.W., de Boer, T., Langenberg, D.M.L., Hoeve, M.A., Kramer, M., Vaisberg, E., Kastelein, R., Kolk, A., de Waal-Malefyt, R., and Ottenhoff, T.H.M. (2004). Human IL-23-producing type 1 macrophages promote but IL-10-producing type 2 macrophages subvert immunity to (myco)bacteria. Proc. Natl. Acad. Sci. USA *101*, 4560–4565. https://doi.org/10.1073/pnas.0400983101.
35. Martinez, F.O., Gordon, S., Locati, M., and Mantovani, A. (2006). Transcriptional profiling of the human monocyte-to-macrophage differentiation and polarization: new molecules and patterns of gene expression. J. Immunol. *177*, 7303–7311. https://doi.org/10.4049/jimmunol.177.10.7303.
36. Ushach, I., and Zlotnik, A. (2016). Biological role of granulocyte macrophage colony-stimulating factor (GM-CSF) and macrophage colony-stimulating factor (M-CSF) on cells of the myeloid lineage. J. Leukoc. Biol. *100*, 481–489. https://doi.org/10.1189/jlb.3RU0316-144R.
37. Ohradanova-Repic, A., Machacek, C., Fischer, M.B., and Stockinger, H. (2016). Differentiation of human monocytes and derived subsets of macrophages and dendritic cells by the HLDA10 monoclonal antibody panel. Clin. Transl. Immunology *5*, e55. https://doi.org/10.1038/cti.2015.39.

38. Corcione, A., Tortolina, G., Bonecchi, R., Battilana, N., Taborelli, G., Malavasi, F., Sozzani, S., Ottonello, L., Dallegri, F., and Pistoia, V. (2002). Chemotaxis of human tonsil B lymphocytes to CC chemokine receptor (CCR) 1, CCR2 and CCR4 ligands is restricted to non-germinal center cells. Int. Immunol. *14*, 883–892. https://doi.org/10.1093/intimm/dxf054.

39. Bower, M., and Carbone, A. (2021). KSHV/HHV8-Associated Lymphoproliferative Disorders: Lessons Learnt from People Living with HIV. Hemato *2*, 703–712. https://doi.org/10.3390/hemato2040047.

40. Jourdan, M., Cren, M., Robert, N., Bollore, K., Fest, T., Duperray, C., Guilloton, F., Hose, D., Tarte, K., and Klein, B. (2014). IL-6 supports the generation of human long-lived plasma cells in combination with either APRIL or stromal cell-soluble factors. Leukemia *28*, 1647–1656. https://doi.org/10.1038/leu.2014.61.

41. Benson, M.J., Dillon, S.R., Castigli, E., Geha, R.S., Xu, S., Lam, K.P., and Noelle, R.J. (2008). Cutting edge: the dependence of plasma cells and independence of memory B cells on BAFF and APRIL. J. Immunol. *180*, 3655–3659. https://doi.org/10.4049/jimmunol.180.6.3655.

42. Haiat, S., Billard, C., Quiney, C., Ajchenbaum-Cymbalista, F., and Kolb, J.P. (2006). Role of BAFF and APRIL in human B-cell chronic lymphocytic leukaemia. Immunology *118*, 281–292. https://doi.org/10.1111/j.1365-2567.2006.02377.x.

43. Jourdan, M., Caraux, A., De Vos, J., Fiol, G., Larroque, M., Cognot, C., Bret, C., Duperray, C., Hose, D., and Klein, B. (2009). An in vitro model of differentiation of memory B cells into plasmablasts and plasma cells including detailed phenotypic and molecular characterization. Blood *114*, 5173–5181. https://doi.org/10.1182/blood-2009-07-235960.

44. Matsuda, Y., Haneda, M., Kadomatsu, K., and Kobayashi, T. (2015). A proliferation-inducing ligand sustains the proliferation of human naive (CD27(-)) B cells and mediates their differentiation into long-lived plasma cells in vitro via transmembrane activator and calcium modulator and cyclophilin ligand interactor and B-cell mature antigen. Cell. Immunol. *295*, 127–136. https://doi.org/10.1016/j.cellimm.2015.02.011.

45. Jourdan, M., Cren, M., Schafer, P., Robert, N., Duperray, C., Vincent, L., Ceballos, P., Cartron, G., Rossi, J.F., Moreaux, J., et al. (2016). Differential effects of lenalidomide during plasma cell differentiation. Oncotarget *7*, 28096–28111. https://doi.org/10.18632/oncotarget.8581.

46. Sanz, I., Wei, C., Jenks, S.A., Cashman, K.S., Tipton, C., Woodruff, M.C., Hom, J., and Lee, F.E.H. (2019). Challenges and Opportunities for Consistent Classification of Human B Cell and Plasma Cell Populations. Front. Immunol. *10*, 2458. https://doi.org/10.3389/fimmu.2019.02458.

47. Nalwoga, A., Webb, E.L., Chihota, B., Miley, W., Walusimbi, B., Nassuuna, J., Sanya, R.E., Nkurunungi, G., Labo, N., Elliott, A.M., et al. (2019). Kaposi's sarcoma-associated herpesvirus seropositivity is associated with parasite infections in Ugandan fishing communities on Lake Victoria islands. PLoS Negl. Trop. Dis. *13*, e0007776. https://doi.org/10.1371/journal.pntd.0007776.

48. Hou, N., Jiang, N., Zou, Y., Piao, X., Liu, S., Li, S., and Chen, Q. (2017). Down-Regulation of Tim-3 in Monocytes and Macrophages in Plasmodium Infection and Its Association with Parasite Clearance. Front. Microbiol. *8*, 1431. https://doi.org/10.3389/fmicb.2017.01431.

49. Dobbs, K.R., Embury, P., Vulule, J., Odada, P.S., Rosa, B.A., Mitreva, M., Kazura, J.W., and Dent, A.E. (2017). Monocyte dysregulation and systemic inflammation during pediatric falciparum malaria. JCI Insight *2*, e95352. https://doi.org/10.1172/jci.insight.95352.

50. van Wolfswinkel, M.E., Langenberg, M.C.C., Wammes, L.J., Sauerwein, R.W., Koelewijn, R., Hermsen, C.C., van Hellemond, J.J., and van Genderen, P.J. (2017). Changes in total and differential leukocyte counts during the clinically silent liver phase in a controlled human malaria infection in malaria-naive Dutch volunteers. Malar. J. *16*, 457. https://doi.org/10.1186/s12936-017-2108-1.

51. Antwi-Baffour, S., Kyeremeh, R., Buabeng, D., Adjei, J.K., Aryeh, C., Kpentey, G., and Seidu, M.A. (2018). Correlation of malaria parasitaemia with peripheral blood monocyte to lymphocyte ratio as indicator of susceptibility to severe malaria in Ghanaian children. Malar. J. *17*, 419. https://doi.org/10.1186/s12936-018-2569-x.

52. Passos, L.S.A., Gazzinelli-Guimarães, P.H., Oliveira Mendes, T.A.d., Guimarães, A.C.G., Silveira Lemos, D.D., Ricci, N.D., Gonçalves, R., Bartholomeu, D.C., Fujiwara, R.T., and Bueno, L.L. (2017). Regulatory monocytes in helminth infections: insights from the modulation during human hookworm infection. BMC Infect. Dis. *17*, 253. https://doi.org/10.1186/s12879-017-2366-0.

53. Agbolade, O., Akinboye, D., and Ogunkolo, O. (2005). Loa loa and Mansonella perstans: Neglected human infections that need control in Nigeria. Afr. J. Biotechnol. *4*, 1554–1558.

54. Nascimento, M., Huang, S.C., Smith, A., Everts, B., Lam, W., Bassity, E., Gautier, E.L., Randolph, G.J., and Pearce, E.J. (2014). Ly6Chi monocyte recruitment is responsible for Th2 associated host-protective macrophage accumulation in liver inflammation due to schistosomiasis. PLoS Pathog. *10*, e1004282. https://doi.org/10.1371/journal.ppat.1004282.

55. Vieira, J., Huang, M.L., Koelle, D.M., and Corey, L. (1997). Transmissible Kaposi's sarcoma-associated herpesvirus (human herpesvirus 8) in saliva of men with a history of Kaposi's sarcoma. J. Virol. *71*, 7083–7087.

56. Merry, R., Belfield, L., McArdle, P., McLennan, A., Crean, S., and Foey, A. (2012). Oral health and pathology: a macrophage account. Br. J. Oral Maxillofac. Surg. *50*, 2–7. https://doi.org/10.1016/j.bjoms.2010.10.020.

57. Faure, A., Hayes, M., and Sugden, B. (2019). How Kaposi's sarcoma-associated herpesvirus stably transforms peripheral B cells towards lymphomagenesis. Proc. Natl. Acad. Sci. USA *116*, 16519–16528. https://doi.org/10.1073/pnas.1905025116.

58. Blackbourn, D.J., Lennette, E., Klencke, B., Moses, A., Chandran, B., Weinstein, M., Glogau, R.G., Witte, M.H., Way, D.L., Kutzkey, T., et al. (2000). The restricted cellular host range of human herpesvirus 8. AIDS *14*, 1123–1133.

59. McHugh, D., Caduff, N., Barros, M.H.M., Rämer, P.C., Raykova, A., Murer, A., Landtwing, V., Quast, I., Styles, C.T., Spohn, M., et al. (2017). Persistent KSHV Infection Increases EBV-Associated Tumor Formation In Vivo via Enhanced EBV Lytic Gene Expression. Cell Host Microbe *22*, 61–73.e7. https://doi.org/10.1016/j.chom.2017.06.009.

60. Morillon, Y.M., 2nd, Sabzevari, A., Schlom, J., and Greiner, J.W. (2020). The Development of Next-generation PBMC Humanized Mice for Preclinical Investigation of Cancer Immunotherapeutic Agents. Anticancer Res. *40*, 5329–5341. https://doi.org/10.21873/anticanres.14540.

61. Roughan, J.E., and Thorley-Lawson, D.A. (2009). The intersection of Epstein-Barr virus with the germinal center. J. Virol. *83*, 3968–3976. https://doi.org/10.1128/JVI.02609-08.

62. Collins, C.M., and Speck, S.H. (2012). Tracking murine gammaherpesvirus 68 infection of germinal center B cells in vivo. PLoS One *7*, e33230. https://doi.org/10.1371/journal.pone.0033230.

63. Frederico, B., Milho, R., May, J.S., Gillet, L., and Stevenson, P.G. (2012). Myeloid infection links epithelial and B cell tropisms of Murid Herpesvirus-4. PLoS Pathog. *8*, e1002935. https://doi.org/10.1371/journal.ppat.1002935.

64. Blasig, C., Zietz, C., Haar, B., Neipel, F., Esser, S., Brockmeyer, N.h., Tschachler, E., Colombini, S., Ensoli, B., and Stürzl, M. (1997). Monocytes in Kaposi's sarcoma Lesions Are Productively Infected by Human Herpesvirus 8. J. Virol. *71*, 7963–7968.

65. Host, K.M., Jacobs, S.R., West, J.A., Zhang, Z., Costantini, L.M., Stopford, C.M., Dittmer, D.P., and Damania, B. (2017). Kaposi's Sarcoma-Associated Herpesvirus Increases PD-L1 and Proinflammatory Cytokine Expression in Human Monocytes. mBio *8*, e00917. https://doi.org/10.1128/mBio.00917-17.

66. Nduati, E., Gwela, A., Karanja, H., Mugyenyi, C., Langhorne, J., Marsh, K., and Urban, B.C. (2011). The plasma concentration of the B cell activating factor is increased in children with acute malaria. J. Infect. Dis. *204*, 962–970. https://doi.org/10.1093/infdis/jir438.

67. Scholzen, A., Teirlinck, A.C., Bijker, E.M., Roestenberg, M., Hermsen, C.C., Hoffman, S.L., and Sauerwein, R.W. (2014). BAFF and BAFF receptor levels correlate with B cell subset activation and redistribution in controlled human malaria infection. J. Immunol. *192*, 3719–3729. https://doi.org/10.4049/jimmunol.1302960.

68. Besnard, A.G., Guabiraba, R., Niedbala, W., Palomo, J., Reverchon, F., Shaw, T.N., Couper, K.N., Ryffel, B., and Liew, F.Y. (2015). IL-33-mediated protection against experimental cerebral malaria is linked to induction of type 2 innate lymphoid cells, M2 macrophages and regulatory T cells. PLoS Pathog. *11*, e1004607. https://doi.org/10.1371/journal.ppat.1004607.

69. Weinberg, J.B., Volkheimer, A.D., Rubach, M.P., Florence, S.M., Mukemba, J.P., Kalingonji, A.R., Langelier, C., Chen, Y., Bush, M., Yeo, T.W., et al. (2016). Monocyte polarization in children with falciparum malaria: relationship to nitric oxide insufficiency and disease severity. Sci. Rep. *6*, 29151. https://doi.org/10.1038/srep29151.

70. Wallace, L., Henkin, R., and Mathies, A.W. (1956). Trichostrongylus infestation with profound eosinophilia. Ann. Intern. Med. *45*, 146–150. https://doi.org/10.7326/0003-4819-45-1-146.

71. Butler, L.M., Neilands, T.B., Mosam, A., Mzolo, S., and Martin, J.N. (2010). A population-based study of how children are exposed to saliva in KwaZulu-Natal Province, South Africa: implications for the spread of saliva-borne pathogens to children. Trop. Med. Int. Health *15*, 442–453. https://doi.org/10.1111/j.1365-3156.2010.02474.x.

72. Olp, L.N., Minhas, V., Gondwe, C., Poppe, L.K., Rogers, A.M., Kankasa, C., West, J.T., and Wood, C. (2016). Longitudinal analysis of the humoral response to Kaposi's sarcoma-associated herpesvirus after primary infection in children. J. Med. Virol. *88*, 1973–1981. https://doi.org/10.1002/jmv.24546.

73. Gilardini Montani, M.S., Falcinelli, L., Santarelli, R., Granato, M., Romeo, M.A., Cecere, N., Gonnella, R., D'Orazi, G., Faggioni, A., and Cirone, M. (2020). KSHV infection skews macrophage polarisation towards M2-like/TAM and activates Ire1 alpha-XBP1 axis up-regulating pro-tumorigenic cytokine release and PD-L1 expression. Br. J. Cancer *123*, 298–306. https://doi.org/10.1038/s41416-020-0872-0.

74. Bhaskaran, N., Ghosh, S.K., Yu, X., Qin, S., Weinberg, A., Pandiyan, P., and Ye, F. (2017). Kaposi's sarcoma-associated herpesvirus infection promotes differentiation and polarization of monocytes into tumor-associated macrophages. Cell Cycle *16*, 1611–1621. https://doi.org/10.1080/15384101.2017.1356509.

75. Lee, S.H., Starkey, P.M., and Gordon, S. (1985). Quantitative analysis of total macrophage content in adult mouse tissues. Immunochemical studies with monoclonal antibody F4/80. J. Exp. Med. *161*, 475–489. https://doi.org/10.1084/jem.161.3.475.

76. Isidro, R.A., and Appleyard, C.B. (2016). Colonic macrophage polarization in homeostasis, inflammation, and cancer. Am. J. Physiol. Gastrointest. Liver Physiol. *311*, G59-G73. https://doi.org/10.1152/ajpgi.00123.2016.

77. Kurashina, R., Denda-Nagai, K., Saba, K., Hisai, T., Hara, H., and Irimura, T. (2021). Intestinal lamina propria macrophages upregulate interleukin-10 mRNA in response to signals from commensal bacteria recognized by MGL1/CD301a. Glycobiology *31*, 827–837. https://doi.org/10.1093/glycob/cwab015.

78. Kelley, C.F., Kraft, C.S., de Man, T.J., Duphare, C., Lee, H.W., Yang, J., Easley, K.A., Tharp, G.K., Mulligan, M.J., Sullivan, P.S., et al. (2017). The rectal mucosa and condomless receptive anal intercourse in HIV-negative MSM: implications for HIV transmission and prevention. Mucosal Immunol. *10*, 996–1007. https://doi.org/10.1038/mi.2016.97.

79. Beral, V., Bull, D., Darby, S., Weller, I., Carne, C., Beecham, M., and Jaffe, H. (1992). Risk of Kaposi's sarcoma and sexual practices associated with faecal contact in homosexual or bisexual men with AIDS. Lancet *339*, 632–635. https://doi.org/10.1016/0140-6736(92)90793-3.

80. Butler, L.M., Osmond, D.H., Jones, A.G., and Martin, J.N. (2009). Use of saliva as a lubricant in anal sexual practices among homosexual men. J. Acquir. Immune Defic. Syndr. *50*, 162–167. https://doi.org/10.1097/QAI.0b013e31819388a9.

81. Chan, S.R., Bloomer, C., and Chandran, B. (1998). Identification and characterization of human herpesvirus-8 lytic cycle-associated ORF 59 protein and the encoding cDNA by monoclonal antibody. Virology *240*, 118–126. https://doi.org/10.1006/viro.1997.8911.

82. Myoung, J., and Ganem, D. (2011). Generation of a doxycycline-inducible KSHV producer cell line of endothelial origin: maintenance of tight latency with efficient reactivation upon induction. J. Virol. Methods *174*, 12–21. https://doi.org/10.1016/j.jviromet.2011.03.012.

83. WHO (2021). WHO Malaria Terminology, 2021 Update (WHO).

STAR★METHODS

KEY RESOURCES TABLE

REAGENT or RESOURCE	SOURCE	IDENTIFIER
Antibodies		
CD3-PerCP-Cy5.5	BD Biosciences	Cat#560835, RRID:AB_2033956
CD4-BV786	BD Biosciences	Cat#563881, RRID:AB_2738463
CD8-PE-Cy7	BD Biosciences	Cat#560917, RRID:AB_2033970
CD14-BV711	BD Biosciences	Cat#563372, RRID:AB_2744290
CD14-AlexaFluor700	eBioscience	Cat#56-0149-41, RRID:AB_2574496
CD19-BUV395	BD Biosciences	Cat#563551, RRID:AB_2738274
CD38-BV421	BD Biosciences	Cat#562444, RRID:AB_11151894
CD38-BB700	BD Biosciences	Cat#566445, RRID:AB_2744375
CD56-APC	eBioscience	Cat#17-0566-41, RRID:AB_2573147
CD138-APC	eBioscience	Cat#17-1389-42, RRID:AB_11218892
anti-LANA LN53 rat	Millipore	Cat# MABE1109, RRID:AB_2860565
anti-ORF59 11D1 mouse	From Chan, S.R., et al. (1998)[81]	N/A
goat anti-rat Alexa Fluor 488	Invitrogen	Cat#A11006, RRID:AB_2534074
goat anti-rat Alexa Fluor 647	Invitrogen	Cat#A21247, RRID:AB_141778
goat anti-mouse Alexa Fluor 647	Invitrogen	Cat#A32728, RRID:AB_2633277
CD19 Spark NIR 685 clone: HIB19	BioLegend	Cat# 302270, RRID:AB_2832581
CD14 Spark Blue 550 clone: 63D3	BioLegend	Cat# 367148, RRID:AB_2832724
Bacterial and virus strains		
Virus: KSHV	iSLK.219 (Myoung and Ganem (2011)[82]	N/A
Biological samples		
PBLs, B cells, or monocytes purified from leukodepletion cones obtained from healthy blood donors	Mass General Brigham Crimson Core	N/A
1	Longitudinal study in Kisumu, Kenya between 2019 and 2022 (G.S.-R., S.O., R.R., unpublished data)	N/A
Chemicals, peptides, and recombinant proteins		
human recombinant M-CSF	Stemcell Technologies	Cat#78150
human recombinant GM-CSF	Stemcell Technologies	Cat#78140
human recombinant BAFF	R&D Systems	Cat#7537-BF-025
human recombinant APRIL	R&D Systems	Cat#5860-AP-010
Critical commercial assays		
RosetteSep Human B Cell Enrichment Cocktail	Stemcell Technologies	Cat#15024
EasySep Human B Cell Enrichment Kit	Stemcell Technologies	Cat#19054
EasySep™ Direct Human B Cell Isolation Kit	Stemcell Technologies	Cat#19674
EasySep™ Direct Human Monocyte Isolation Kit	Stemcell Technologies	Cat#19669
CellTrace Violet	Life Technologies	Cat# C34557
BAFF ELISA kit	Abcam	Cat# ab119579
Legend MAX™ Human APRIL ELISA kit	BioLegend	Cat#439307
Quantibody Human Inflammation Array Q3	RayBiotech	Cat# QAH-INF-3-1
Experimental models: Cell lines		
iSLK.219	iSLK.219 Myoung and Ganem (2011)[82]	N/A

(*Continued on next page*)

Continued

REAGENT or RESOURCE	SOURCE	IDENTIFIER
293T	ATCC	Cat# CRL-3216, RRID:CVCL_0063
Software and algorithms		
BD FACS Diva	BD Biosciences	https://www.bdbiosciences.com/en-us/products/software/instrument-software/bd-facsdiva-software
FlowJo v10.7.1 and v9.5.2	TreeStar, Ashland, OR, USA	https://www.flowjo.com/
GraphPad Prism v9.2.0	GraphPad Software Inc.	https://www.graphpad.com
Microsoft Excel v16.5	Microsoft 365	https://www.microsoft.com/en-us/download/details.aspx?id=56547
Zen Blue v2.6	Zeiss	https://www.zeiss.com/microscopy/en/products/software/zeiss-zen.html
RayBiotech Q-Analyzer v8.40.4	RayBiotech	https://www.raybiotech.com/tools/array-analysis-tool/
Other		
Fixable Near-IR Dead	Invitrogen	Cat# L34975
Prolong Gold Antifade with DAPI	Life Technologies	Cat# P36935
Live/Dead fixable blue	Thermo Fisher Scientific	Cat# L23105

RESOURCE AVAILABILITY

Lead contact

Further information and requests for resources and reagents should be directed to and will be fulfilled by the lead contact, Kenneth M. Kaye (kkaye@bwh.harvard.edu).

Materials availability

This study did not generate new unique reagents.

Data and code availability

- All data reported in this paper will be shared by the lead contact upon request.
- This paper does not report original code
- Any additional information required to reanalyze the data reported in this paper is available from the lead contact upon request.

EXPERIMENTAL MODEL AND SUBJECT DETAILS

Human studies

Study subjects were part of a longitudinal study in Kisumu, Kenya between 2019-2022 (G.S.-R., S.O., R.R., unpublished data). Briefly, two groups of children aged 1 to 5 years old were enrolled from Chulaimbo County Hospital, which cares for patients from a malaria-endemic region of Western Kenya: children with uncomplicated malaria (25 female, 24 male), defined as symptomatic malaria parasitemia without signs of severity or evidence of vital organ dysfunction,[83] e.g., evidence of fever >37.5°C, level of parasitemia >5000 parasites/mL by blood smear (BS), and first response malaria Ag *P. falciparum* rapid diagnostic test (RDT) (Abbott, Lake Forest, IL) positivity, and age-and sex-matched children (26 female, 20 male), without evidence of fever or malaria (BS-negative and RDT-negative). This second group served as the control group; participants for this group were recruited from the villages served by the hospital. Children with malaria were given treatment according to Kenyan Ministry of Health guidelines. Hemoglobin (Hgb) levels were determined using a portable B-hemoglobin photometer (Hemocue AB Angelholm, Sweden). Children with severe anemia (Hgb <7), chronic illness (e.g., HIV, or sickle cell disease), or severe neurological disease (e.g., known developmental delay) were not enrolled.

Informed consent was obtained from mothers or guardians of study participants. Protocol and consent forms were approved by the Kenya Medical Research Institute (KEMRI) and the Colorado Multiple Institutional Review Board (COMIRB).

Primary cells

PBLs, B cells, or monocytes were purified from leukodepletion cones obtained from healthy blood donors (51 donor samples) from Mass General Brigham Crimson Core. Cells were cultured in Primary cell medium: RPMI 1640 with L-glutamine (Corning, 10-040-CV)

supplemented with 15% FBS (Atlas Biologicals, FP-0050-A), 15 μg/mL gentamicin, and additional 2 mM L-glutamine (Gibco, 25030081). All cells were cultured in humidified incubators at 37°C and 5% CO_2.

Cell lines

293T cells (ATCC CRL-3216) were cultured in DMEM (Dulbecco Modification of Eagle Medium) with 4.5 g/L glucose, L-glutamine, and sodium pyruvate (Corning, 10-013-CV) supplemented with 10% Bovine Growth Serum (BGS) (HyClone, SH3054103) and 15 μg/mL gentamicin (Gemini Bio-products, 400-108). Cells were cultured in humidified incubators at 37°C and 5% CO_2. Cells tested negative for mycoplasma.

iSLK.219[82] were maintained in DMEM supplemented with 10% BGS, 15 μg/mL gentamicin, 8 μg/mL puromycin (Invitrogen, ant-pr-1) and 250 μg/mL G418 (Gemini Bio-Products, 400-113). Cells were cultured in humidified incubators at 37°C and 5% CO_2. Cells tested negative for mycoplasma.

METHOD DETAILS

PBL isolation

PBLs were purified by layering cone contents diluted 1:1 with PBS on Lymphoprep (Stemcell Technologies, 07811) followed by centrifugation at 400 rcf for 30 min at room temperature with the brake off. After centrifugation, the mononuclear leukocyte layer was collected, washed twice using RPMI medium and strained through a 70 μm cell strainer (Corning, 431751) to remove any lipid particles.

In the initial experiments, B cells were purified in two sequential steps (unless specified "enriched," in which case only the first step used) by negative selection, first using RosetteSep Human B Cell Enrichment Cocktail (Stemcell Technologies, 15024) according to the manufacturer's instructions, and then using EasySep Human B Cell Enrichment Kit (Stemcell Technologies, 19054) according to the manufacturer's instructions except that 1/5 volumes of reagents were used due to the use of enriched B cells. After purification, cells obtained were routinely ≥95% positive for CD19 (Figure S1A). Later in the work, B cells were purified by negative selection using EasySep Direct Human B Cell Isolation Kit (Stemcell Technologies, 19674) according to the manufacturer's instructions. After purification, cells obtained were routinely ≥98% positive for CD19 (Figure S1A).

Monocytes were purified by negative selection using EasySep™ Direct Human Monocyte Isolation Kit (Stemcell Technologies, 19669) according to the manufacturer's instructions.

Differentiation of monocytes into macrophages

Monocytes, purified by negative selection from leukodepletion cones, were either first stored at −140°C, or freshly plated in 24-well plates at 10^6 cells per well in Primary cell medium with addition of either 50 ng/mL human recombinant M-CSF (Stemcell Technologies, 78150) or 50 ng/mL human recombinant GM-CSF (Stemcell Technologies, 78140). After 3 days, the medium was exchanged for fresh medium supplemented with M-CSF or GM-CSF and subsequently, fresh medium with M-CSF or GM-CSF exchanged every 2 days. Macrophages were considered fully differentiated after 7 days from the start of differentiation and were maintained in medium with M-CSF or GM-CSF throughout the experiments.

Virus production and titration

iSLK.219 cells, containing recombinant KSHV derived from an infected human primary effusion lymphoma cell line,[82] were induced with 1 μg/mL doxycycline (Sigma, D9891-1G) and 1mM sodium butyrate (Alfa Aesar, A1107922) in medium without puromycin and G418 for 4 days. Supernatant was then harvested and collected by centrifugation at 300 rcf for 5 min to remove cell debris. Supernatant was filtered through 0.45 μm cellulose acetate filters (low protein binding) (Corning, 430514), and concentrated by ultracentrifugation at 25,000 rpm for 2h at 4°C in sterile 38 mL tubes (Beckman Coulter, C14301), using an SW28 Beckman Coulter rotor and Sorvall Discovery 90SE ultracentrifuge. The supernatant was removed, and tubes left inverted on sterile tissue paper for 5-10 min to remove remaining liquid. Subsequently, 350 μL (1/100 of starting volume) of Primary cell medium was added to each tube, tubes were transferred into sterile conical 50 mL tubes (Corning, 430829), and pellets left to resuspend by gentle shaking at 4°C, overnight. Virus titer was determined using serial 10-fold dilutions (1:10 to 1:1,000,000) of virus, of which 1 mL of each dilution was used to infect 10^5 293T cells in 24-well plates. The number of GFP expressing (infected) 293T cells per well at 48h pi was then determined by fluorescence microscopy.

Flow cytometry staining and gating

Where indicated, cells were stained with CellTrace Violet (Life Technologies, C34557) according to the manufacturer's instructions before infection with KSHV. Incubations with antibody or stain were performed at indicated time points post infection. Harvested cells ($\sim 10^5$- 10^6) were collected by centrifugation for 4 min at 400 rcf using a microcentrifuge, washed with PBS containing 0.5% BSA (Sigma, A3294-10G), and stained with 1 μL/mL of Fixable Near-IR Dead cell stain (Invitrogen, L34975) in PBS for 15 min in the dark. After washing, cells were blocked with 50 μg of human IgG (Sigma, I4506-10MG) for 10 min, in the dark. After blocking, 90 μL of PBS containing 0.5% BSA with 5 μL of each antibody was incubated with cells for 30 min at 4°C in the dark. Antibodies used were: CD3-PerCP-Cy5.5 (BD Biosciences, 560835), CD4-BV786 (BD Biosciences, 563881), CD8-PE-Cy7 (BD Biosciences,

560917), CD14-BV711 (BD Biosciences, 563372), CD14-AlexaFluor700 (eBioscience, 56-0149-41), CD19-BUV395 (BD Biosciences, 563551), CD38-BV421 (BD Biosciences, 562444), CD38-BB700 (BD Biosciences, 566445), CD56-APC (eBioscience, 17-0566-41), CD138-APC (eBioscience, 17-1389-42). Cells were washed once with PBS containing 0.5% BSA and fixed in 4% PFA (Thermo Scientific, 28906) for 15 min, in the dark. Cells were then washed again once, resuspended in 300 μL PBS containing 0.5% BSA, transferred to 5 mL tubes through a cell strainer (Falcon, 352235), and run on either flow cytometer BD FACSymphony or BD LSRFortessa. The data was analyzed using FlowJo software. The gating strategy (unless specified otherwise) was as follows: debris was first removed using side scatter area (SSC-A) vs. forward scatter area (FSC-A), doublets were excluded using side scatter width (SSC-W) vs. side scatter height (SSC-H), and then dead cells removed using Live/Dead cell stain signal vs. FSC-A. Live cells were analyzed for CellTrace staining, GFP expression (infected cells) or cell surface markers (Figure S3J). Total cell numbers were assessed in experiments by running the entire samples on the flow cytometer, and using FlowJo software to determine the count indicated in appropriate gates.

Immunofluorescence microscopy

Monocytes (10^5/well) were differentiated into macrophages using M-CSF in a 12-well sterile removable chamber attached to a glass slide (Ibidi, 81201). After 7 days of differentiation, macrophages were infected with KSHV or mock-infected. At day 3 pi, media was gently removed from the chambers, and cells were gently washed once with PBS. After washing, cells were fixed in 4% PFA (Thermo Scientific, 28906) for 15 min and washed once with PBS. After fixing, cells were incubated with 100 μL of blocking/permeabilization buffer (PBS containing 10% FCS, 100 mM Glycine, 0.2% Triton X-100) with the addition of 5 μg of human IgG (Sigma, I4506-10MG) per well, for 30 min at room temperature. Primary antibody (anti-LANA LN53 rat (Millipore, MABE1109) 1:200, or anti-ORF59 11D1 mouse[81] (kind gift of Bala Chandran) 1:5) in blocking/permeabilization buffer was then added and incubation performed for 1 h at room temperature. Antibody was then removed, cells washed twice with PBS, and appropriate secondary fluorescent antibody (goat anti-rat Alexa Fluor 488 (Invitrogen, A11006), goat anti-rat Alexa Fluor 647 (Invitrogen, A21247), or goat anti-mouse Alexa Fluor 647 (Invitrogen, A32728)) at 1:1000 in blocking/permeabilization buffer added, followed by incubation for 1 h at room temperature in the dark. Antibody was then removed and cells were washed twice with PBS. After washing, the chamber was detached from the slide and a coverslip mounted using Prolong Gold Antifade with DAPI (Life Technologies, P36935), and left for 24 h in the dark to solidify. Images were taken using a Zeiss LSM800×confocal microscope, 63× objective and Zen Blue software.

Purified B cells co-cultured in the upper chambers of transwells with M-CSF macrophages were removed on day 6 post infection and plated at ~10^5 cells/well in a 12-well sterile removable chamber attached to a glass slide (Ibidi, 81201), previously coated with poly-D-lysine (1 mg/mL). B cells were incubated in the chamber for 1h to allow for attachment and then fixed and stained following the protocol above.

Cytokine detection assays

Monocytes were differentiated into macrophages using M-CSF in 24-well plates for 7 days. KSHV at MOI~1 (or control medium) was added to cells and incubation performed for 7h at 37°C. Virus (or medium) was then removed, cells were washed 1-2x with medium, and then 1 mL of fresh medium with M-CSF added. After 3 days, supernatant was removed and cleared by centrifugation twice at 400 rcf for 4 min to remove cell debris. Cytokine levels were then assessed. The levels of BAFF were assessed following 4 fold dilution of supernatant in duplicate using human BAFF ELISA kit (Abcam, ab119579) according to the manufacturer's instructions. The data were analyzed against a standard curve generated by the absorbance values produced from serially diluted BAFF standards. The levels of APRIL were also assessed following 4 fold dilution of supernatant and Legend MAX™ Human APRIL ELISA Kit (BioLegend, 439307) according to the manufacturer's instructions. Data were analyzed against a standard curve generated by the absorbance values produced by serially diluted APRIL standards. All other cytokines levels were measured using supernatant diluted 4 fold and Quantibody Human Inflammation Array Q3 (RayBiotech, QAH-INF-3-1) according to the manufacturer's instructions. Medium with M-CSF (incubated in parallel for 3 days in one well without macrophages) was used as a control for cytokines that may be present either in medium or FBS. After performing the assay, dried array slides were packed according to the manufacturer's instructions and shipped to RayBiotech to be read using a fluorescence laser scanner. Data were analyzed using RayBiotech (Q-Analyzer v8.40.4) software.

Virus infections of cells and co-cultures

Unless specified otherwise, infections of purified B cells (10^6/well) were performed in 24-well plates in 1 mL of total volume per well with KSHV MOI~1–2. For co-culture experiments, 10^6 B cells were added to 10^6 monocytes or ~10^6 macrophages in wells of a 24-well plate and then virus at MOI~1–2 was added to the co-culture.

For transwell experiments, 10^6 B cells were plated in the bottom compartment, and 10^6 monocytes were plated in the upper compartment with 0.4 μm pore polycarbonate membranes (Corning, 3413) to allow soluble factors and virus (but not cells) access to the lower compartment. KSHV was then added (proportionately by volume) to the upper and lower chambers. Cells were then incubated for the indicated times (usually 5 days), and assayed using flow cytometry.

For the six-week experiment (Figure 5), due to slow infected macrophage cell death, cells were transferred weekly to fresh M-CSF macrophages (differentiated from the same monocyte donor); these macrophages were KSHV infected at MOI~0.5 one day prior to the cell transfer.

To assess possible virus transfer from infected macrophages to B cells, uninfected B cells were plated alone (or infected with KSHV at MOI = 1 as a positive control) or with either mock-infected or KSHV-infected (MOI = 0.5) M-CSF differentiated macrophages, that were infected one day in advance to mimic the conditions in the six-week experiment. After 3 days of co-culture B cells were analyzed for the percentage of infection using flow cytometry.

Cytokine stimulation assays

Mock-infected or KSHV-infected (MOI∼1) B cells (10^6/well in 0.5 mL of Primary cell medium in 48 well plates) were either left unstimulated or were stimulated with 10 ng/mL recombinant human BAFF protein (R&D Systems, 7537-BF-025), 100 ng/mL recombinant human APRIL protein (R&D Systems, 5860-AP-010), or both. The medium with fresh cytokines was exchanged every 2 days and B cells were analyzed by flow cytometry at day 5 post infection.

Assessment of KSHV production from infected macrophages

M-CSF differentiated macrophages at 10^5 cells per well in 96-well plates were incubated with KSHV at MOI∼2 for 4 h at 37°C. Cells were then washed twice with PBS. Seven wells were replenished with 200 μL of fresh medium. In addition, 7 wells were replenished with 200 μL of medium containing 50 μM cidofovir (Sigma-Aldrich, C5874-10MG) to inhibit viral replication, allowing experiments to distinguish residual virus from newly replicated virus. All supernatant from one well for each condition was harvested each day for 7 days. The supernatant was cleared by centrifugation at 400 rcf for 4 min, and stored at 4°C until all time points were harvested. The supernatant was then incubated with 293T cells plated at 10^5 cells per well in 48-well plates. Two days after infection, GFP expressing cells were counted by fluorescence microscopy.

Collection and assessment of PBLs from Kenya

For each participant, venous blood samples were collected in EDTA vacutainers (Becton Dickinson, Franklin Lakes, NJ). Blood was processed by Ficoll- Hypaque density gradient to isolate PBLs. Samples were stored in liquid nitrogen and shipped on dry ice to University of Colorado for further processing.

PBLs were thawed and washed with complete RPMI 1640 medium prior to staining. After washing, cells were resuspended in flow buffer containing phosphate buffered saline, 1% BSA, and 0.1% sodium azide, and counted using a hemocytometer; one million viable cells were stained for flow cytometry. Cells were first stained for viability using Live/Dead fixable blue dye (Thermo Fisher Scientific, Waltham, MA) as per manufacturer's instructions. Cells were then blocked for 10 min at 4°C with 100 μL of a 1:100 diluted Fc blocking reagent (eBioscience, San Diego, CA) in 30 μL flow buffer. After that, cells were incubated with an antibody cocktail containing CD19 Spark NIR 685 clone: HIB19 (Biolegend) and CD14 Spark Blue 550 clone: 63D3 (Biolegend) antibodies. Incubation was performed for 30 min in the dark at 4°C. Cells were then fixed in 500 μL of Fluorofix (Biolegend, San Diego, CA). Samples were run on a Cytek® Aurora (Cytek Bioscience, Fremont, CA) equipped with 5 lasers. Data were analyzed using FlowJo version 9.5.2 (Tress Star, Ashland, OR).

QUANTIFICATION AND STATISTICAL ANALYSIS

Statistical analyses were performed with GraphPad Prism v9.2.0 software and Microsoft Excel v16.5. Tests used and the number of repetitions (n) are indicated in each figure legend. Data are presented either as the mean ± SEM (for the analysis of malaria vs. control groups) or as means ± standard deviation (for all other results). $p < 0.05$ was defined as significant.

Cell Reports, Volume *42*

Supplemental information

Macrophages drive KSHV B cell latency

Agnieszka Szymula, Gabriela Samayoa-Reyes, Sidney Ogolla, Bing Liu, Shijun Li, Athira George, Nicholas Van Sciver, Rosemary Rochford, J. Pedro Simas, and Kenneth M. Kaye

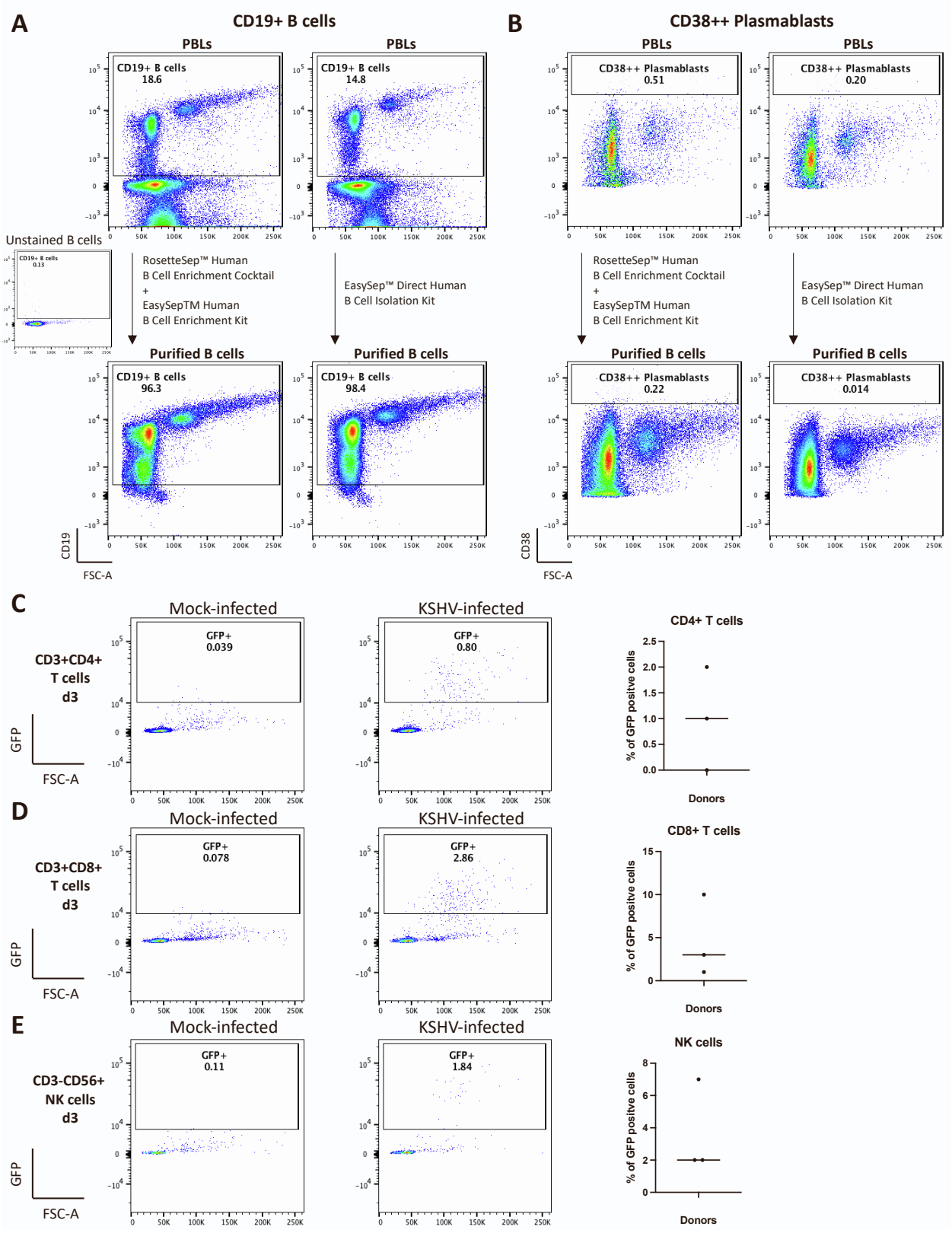

Figure S1. Purification of B cells, and inefficient T cell and NK cell infection by KSHV, related to Figures 1, 2, 4, 5

(A) Percentage of CD19+ B cells before or after purification with different B cell isolation kits.

(B) Percentage of CD19+CD38++ plasmablasts before or after purification with different B cell isolation kits.

(C-E) PBLs from healthy donors were incubated with KSHV (or mock infected), gated for (C) CD4+ T cells, (D) CD8+ T cells, or (E) NK cells and analyzed for infection as determined by viral GFP expression assessed by flow cytometry at day 3 post infection. Data representative of 3 independent experiments with donor samples using infection with MOI~1-5. Percentage of cells expressing GFP are shown at right. Horizontal line indicates median.

See also Figures 1, 2, 4, 5.

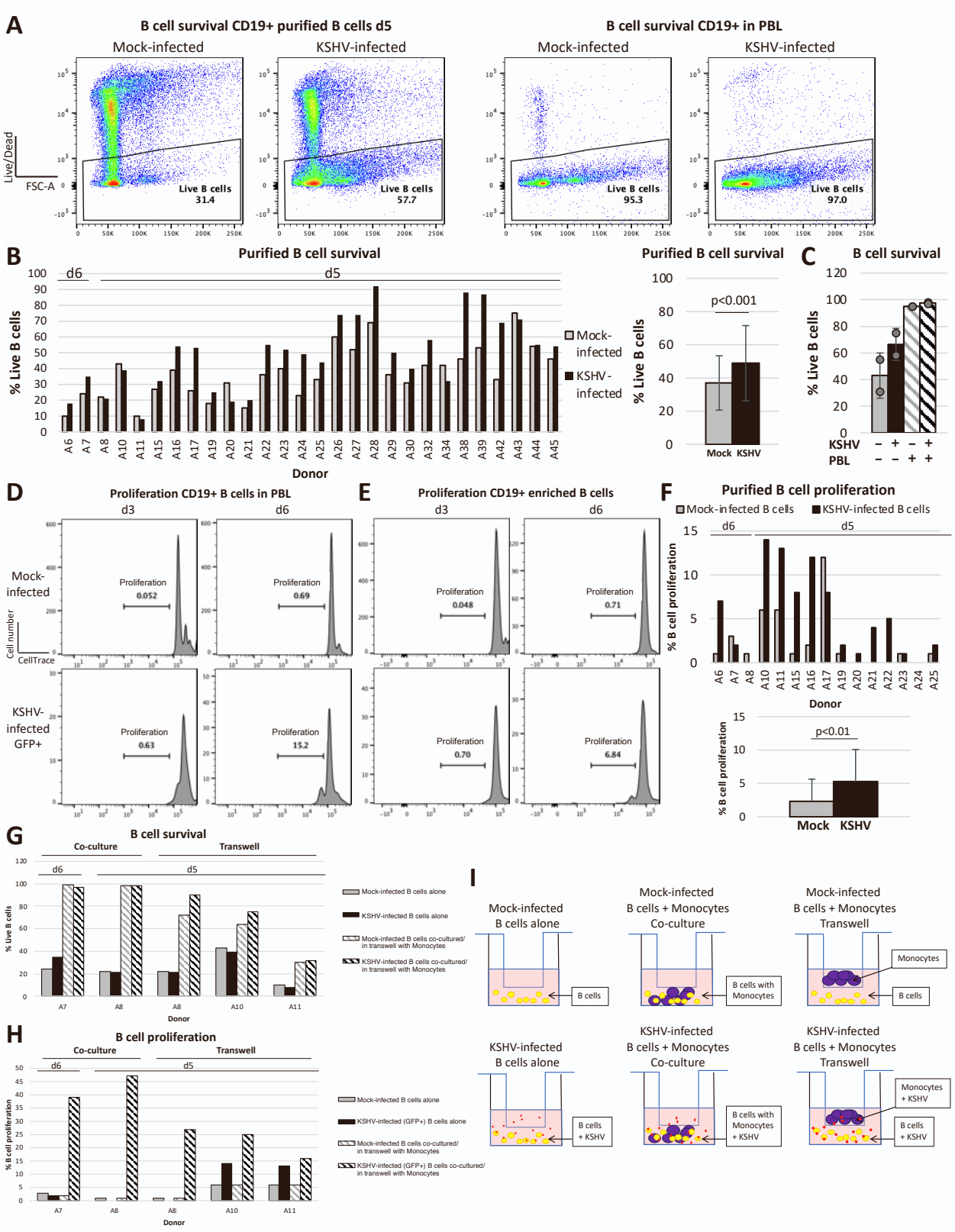

Figure S2. KSHV, PBL or monocyte co-culture increases B cell survival and infected cell

proliferation, related to Figure 2

(A) Survival of purified B cells or B cells within PBLs following infection (or mock infection) with KSHV at MOI~1 at day 5 post infection. Data representative of at least 2 independent donor experiments.

(B) Survival of B cells purified from 28 independent donor samples infected with KSHV at MOI~1-3 at day 5 or 6 post infection. Bar graph at right shows average values. Error bars indicate standard deviation. p value was calculated using t-test: one-tailed paired two sample for means.

(C) Average survival of CD19+ B cells at day 5 (including panel A data). Error bars indicate standard deviation.

(D-E) Proliferation of CD19+ B cells within PBLs (D) or following B cell enrichment (E) on day 3 or 6 after KSHV (or mock) infection at MOI~1. Brackets indicate proliferated cells, which have decreased CellTrace content. Proliferated cell percentages are indicated. Plots gated on live CD19+ B cells (mock-infected) or live CD19+GFP+ B cells (KSHV-infected).

(F) Proliferation of B cells purified from 15 independent blood donor samples on day 5 or 6 post infection with KSHV at MOI~1-2. Averaged values are shown below. Error bars indicate standard deviation. p value calculated using t-test: one-tailed paired two sample for means.

(G-H) Percentage of live (G) or proliferated (H) CD19+ B cells at day 5 or 6 post infection with KSHV (or mock infected) at MOI~1. Infected B cells were identified by viral GFP expression. B cells and monocytes for each infection (or mock infection) were from the same donor.

(I) Experimental setup of B cells either co-cultured with monocytes, or separated from monocytes in transwells.

See also Figure 2.

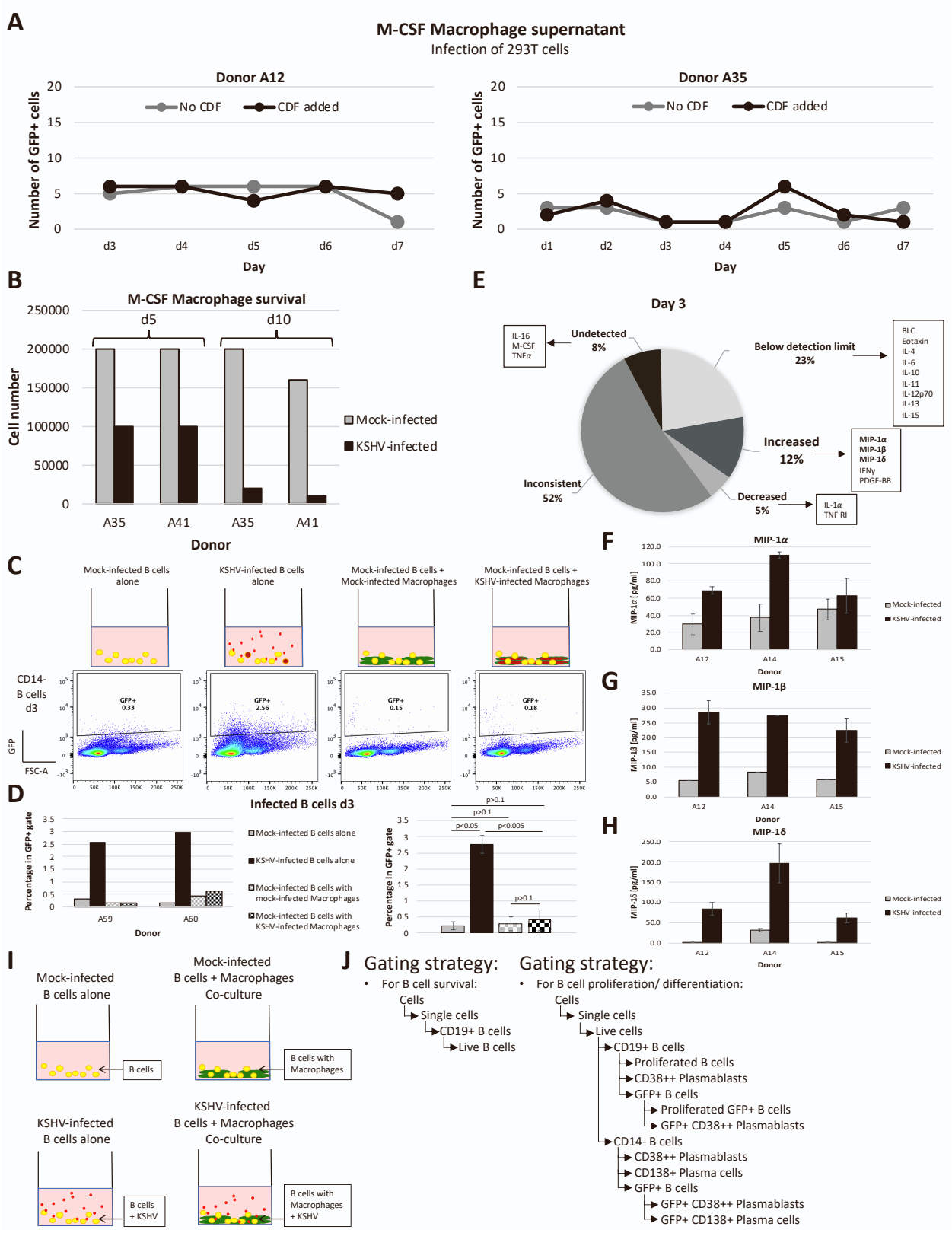

Figure S3. Infected M-CSF macrophages do not produce infectious KSHV, and are induced

for B cell chemoattractants, related to Figure 3

(A) M-CSF-differentiated macrophages from 2 independent donors were infected with KSHV at MOI~2 for 4h and then replenished with fresh medium with or without cidofovir (CDF). Supernatant was then harvested daily and used to infected 293T cells to assess titer of infectious virus. Two days following 293T cell infection, GFP+ (infected) cells were counted using fluorescent microscopy.

(B) Monocytes were M-CSF differentiated into macrophages and infected with KSHV (or mock-infected) at MOI~1. On days 5 and day 10 post infection, macrophages were detached with 5mM EDTA, and live cells assessed by trypan blue.

(C) Purified B cells alone were mock or KSHV-infected, or co cultured with M-CSF macrophages that were infected with KSHV (or mock-infected) one day in advance. After 3 days of co-culture, CD14- B cells were analyzed for percentage of infection as assessed by GFP expression.

(D) Data from 2 independent donors (including panel C data) (left) and average values (right).

(E-H) M-CSF differentiated monocytes were infected with KSHV (or mock-infected) at MOI~1. Supernatant was harvested on day 3 post infection and cytokine levels measured by Quantibody assay.

(E) Pie chart of cytokine changes. “Undetected” indicates no detection following subtraction of levels in blank sample (medium used for macrophage culture). “Below detection limit” indicates cytokines below detection limit as defined by RayBiotech Q-Analyzer v8.40.4.

(F-H) Chemoattractants MIP-1α (F) MIP-1β (G) or MIP-1δ (H) levels determined by Quantibody assay. Error bars indicate standard deviation calculated from four technical replicates (array dots).

(I) Experimental setup of B cell co-culture with macrophages.

(J) Flow cytometry gating strategy.

See also Figure 3.

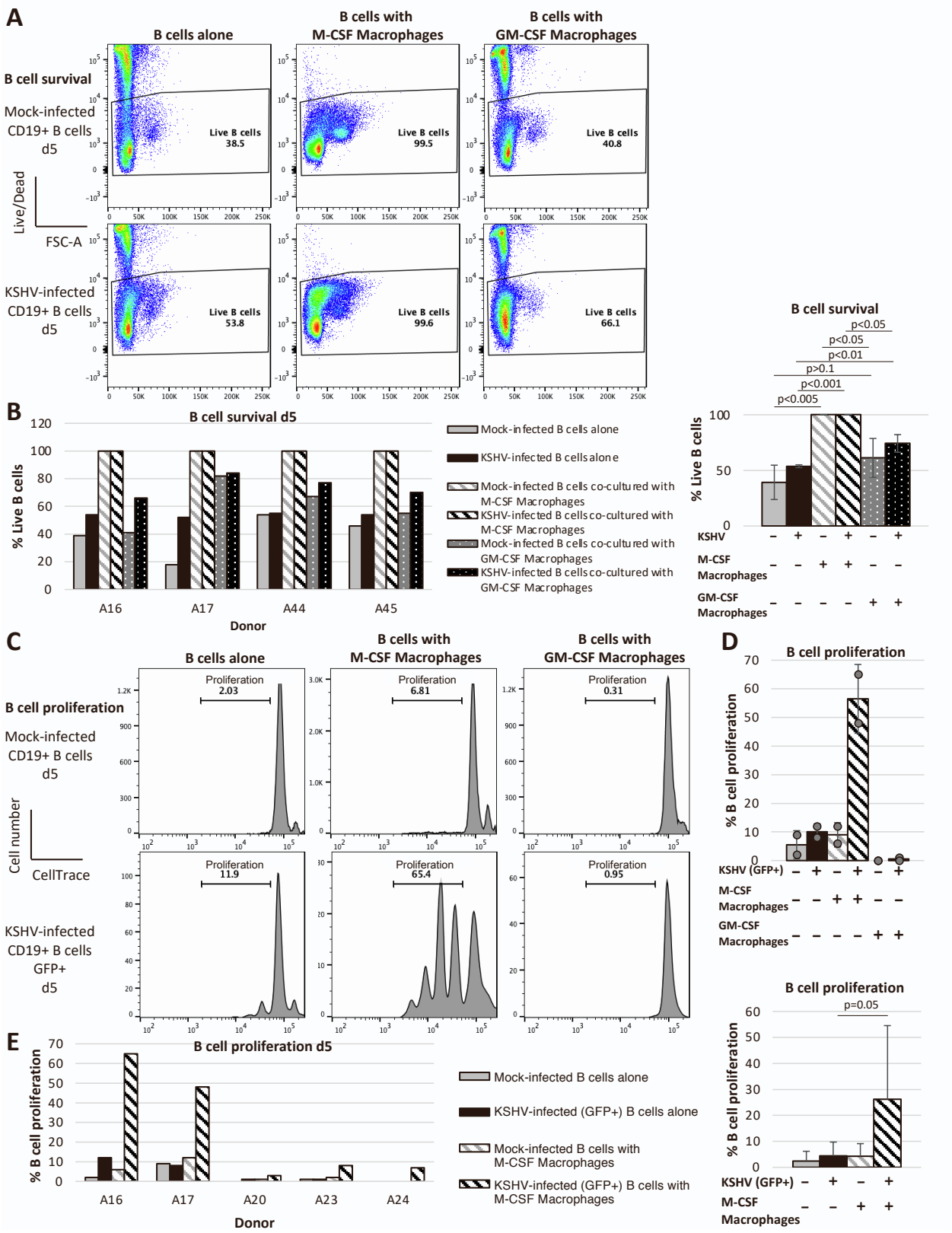

Figure S4. M-CSF differentiated macrophages increase B cell survival and proliferation,

related to Figure 3

(A) Purified B cells alone, or co-cultured with M-CSF or GM-CSF differentiated macrophages were infected with KSHV (or mock infected) at MOI~1-2. At 5 days post infection, B cell survival was assessed by flow cytometry. Plots gated on live CD19+ B cells (mock-infected) or live CD19+GFP+ B cells (KSHV-infected).

(B) B cell survival for 4 independent donor samples. Average values are shown at right. Error bars indicate standard deviation. p values were calculated using t-test: one-tailed paired two sample for means.

(C-E) Purified B cells alone, or co-cultured with M-CSF or GM-CSF differentiated macrophages were infected with KSHV (or mock infected) at MOI~1-2. At 5 days post infection, proliferation was analyzed by flow cytometry. Plots gated on live CD19+ B cells (mock-infected) or live CD19+GFP+ B cells (KSHV-infected). Data are representative of two independent donor experiments, which are presented in panel D.

(E) Percentages of proliferating B cells (including relevant data from panels C and D) at day 5 post infection (or mock infection) with KSHV MOI~1-2. Averages are shown at right. Error bars indicate standard deviation. p value was calculated using t-test: one-tailed paired two sample for means.

See also Figure 3.

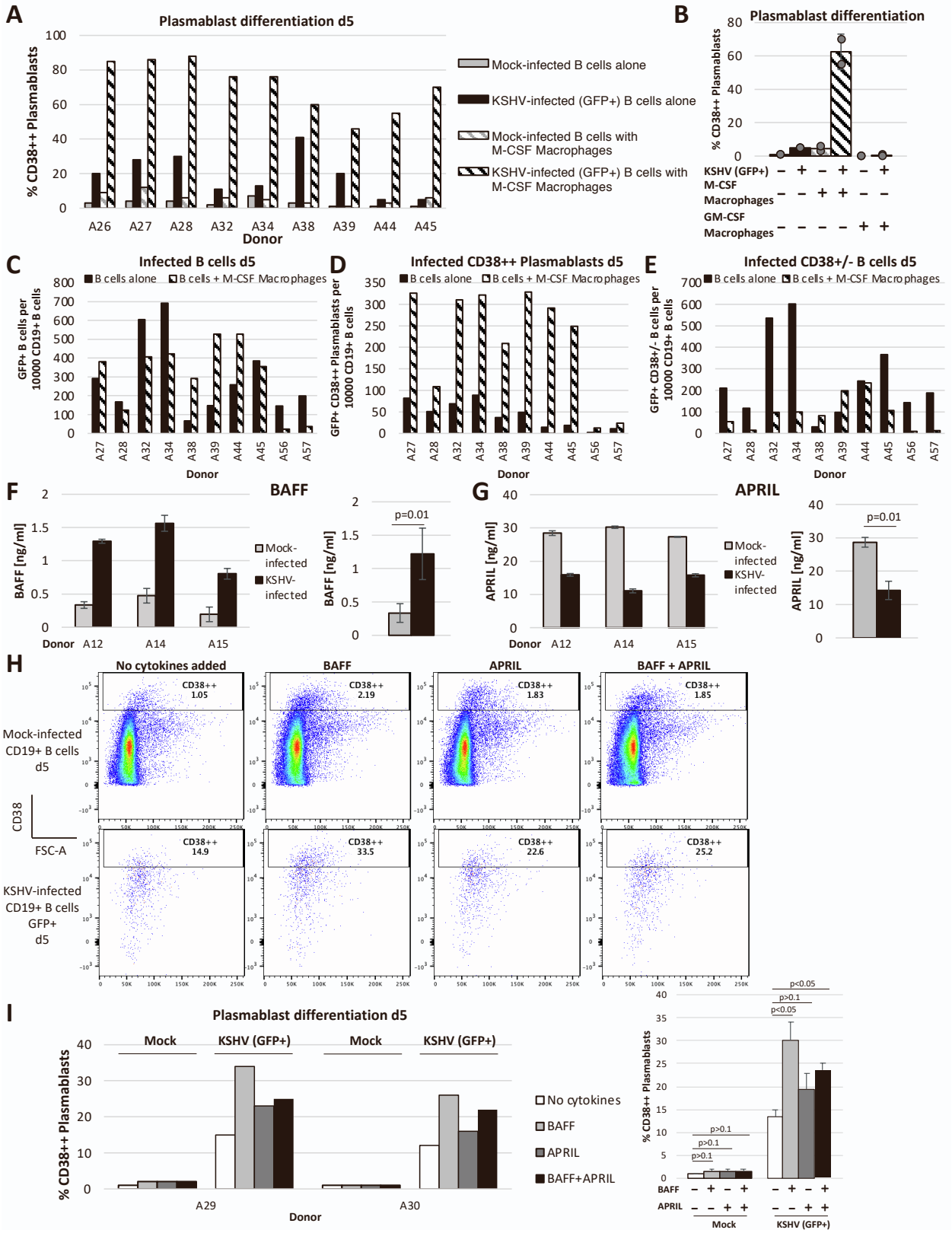

Figure S5. M-CSF, but not GM-CSF, differentiated macrophages drive B cell

differentiation, and KSHV regulates BAFF and APRIL in M-CSF macrophages, related to Figure 4

(A) Purified B cells (9 donor samples) were cultured alone or with M-CSF macrophages and differentiation was assessed by flow cytometry.

(B) Average CD38++ plasmablast differentiation of purified B cells alone, or B cells incubated with M-CSF or GM-CSF macrophages at day 5 post infection (or mock infection) with KSHV MOI~1-2. Error bars indicate standard deviation.

(C-E) Frequencies of infected (GFP+) CD19+ B cells (C), infected CD38++ plasmablasts (D), or infected CD38+/- B cells (E) per 10000 live CD19+ B cells, from 10 independent B cell donor samples on day 5 post infection.

(F-G) Supernatant from M-CSF differentiated macrophages (3 donor samples) infected (or mock-infected) with KSHV at MOI~1 was harvested on day 3 post infection and levels of BAFF (F), APRIL (G) assessed. Error bars indicate standard error from two technical replicates for individual donor samples (at left) or standard deviation for averages (at right). p values were calculated using t-test: paired two sample for means.

(H) Purified B cells were infected (or mock-infected) with KSHV with MOI~1in the presence or absence of cytokines and analyzed by flow cytometry on day 5 post infection for differentiation into CD38++ plasmablasts. Plots gated on live CD19+ B cells (mock-infected) or live CD19+GFP+ B cells (KSHV-infected).

(I) CD38++ plasmablast differentiation at day 5 for individual donor samples with averages shown at right. Error bars indicate standard error. p values were calculated using t-test: one-tailed paired two sample for means.

See also Figure 4.

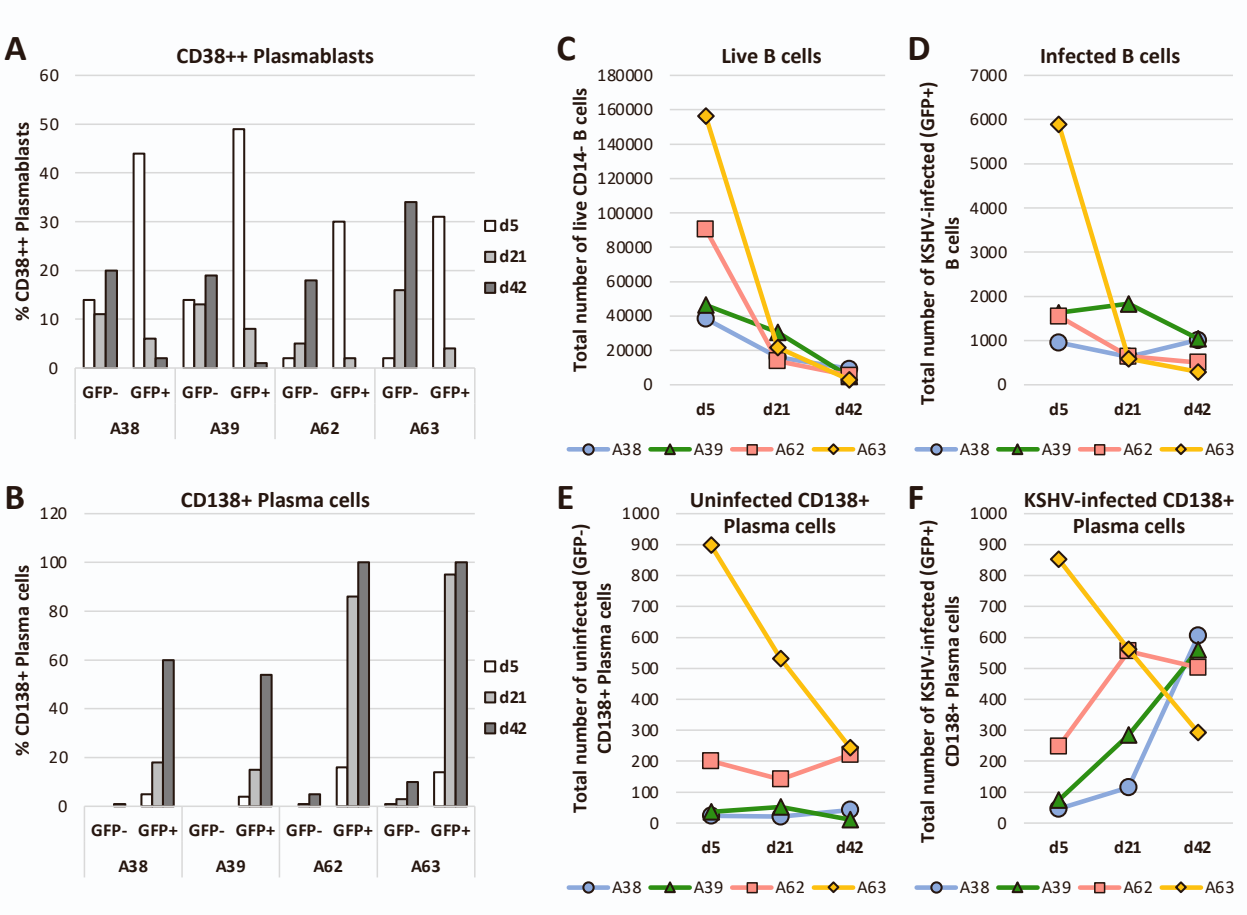

Figure S6. M-CSF macrophages drive KSHV-infected B cell differentiation into long-lived plasma cells, related to Figure 5

(A-F) B cells co-cultured with M-CSF macrophages were infected with KSHV at MOI~1. Due to slow macrophage death, cells were transferred weekly to freshly infected M-CSF macrophages differentiated from the same monocyte donor.

(A-B) Percentages of CD38++ plasmablasts (A) or CD138+ plasma cells (B) from 4 independent donor samples at indicated day post infection with M-CSF macrophage co-culture.

(C-F) Total cell numbers of live B cells (C), infected B cells (D), uninfected plasma cells (E), and KSHV-infected plasma cells (F) from 4 independent donor samples at indicated days post infection.

See also Figure 5.

	Malaria (N=49)	Controls (N=46)	p-value
Age (years)			
Mean (SD)	5.04 (2.2)	4.44 (2.5)	0.22
Sex			
Female	25 (51.0%)	26 (56.5%)	0.66
Male	24 (49.0%)	20 (43.5%)	
Plasmodium load (18S copies/ mL)			
Mean (IQR)	1.35×10^{10} (1.98×10^{7} - 7.09×10^{10})	0 (0)	NA
Hemoglobin (g/dL)			
Mean (SD)	10.47 (2.2)	11.74 (1.5)	0.0017

Table S2. Details of study participants in Kenya, related to Figure 6

95 children (49 with malaria and 46 healthy controls) ages 1-5 years, from the Chulaimbo County Hospital, Chulaimbo, Kenya, were enrolled in the study between 2019 and 2022. Differences in patient characteristics were analyzed using chi-squared tests for categorical data and an unequal variance t-tests for continuous data, as appropriate.

See also Figure 6.